The Pennsylvania State University

The Graduate School

THE ROLE OF ONCOSTATIN M IN EXERCISE-INDUCED DELAYED LATENCY OF BREAST CANCER

A Thesis in

Laboratory Animal Medicine

by

Kara Negrini

Submitted in Partial Fulfillment
of the Requirements
for the Degree of

Master of Science

August 2023

The thesis of Kara Negrini was reviewed and approved by the following:

Kathleen Sturgeon
Assistant Professor of Public Health Sciences
Director of Oncology Nutrition Exercise (ONE) Group
Thesis Advisor

Henry Thompson
Director of Cancer Prevention Laboratory
Colorado State University
Special Signatory

Jenelle Izer
Associate Professor of Comparative Medicine

Tiffany Whitcomb
Professor of Comparative Medicine
Director of Laboratory Animal Medicine Training Program

ABSTRACT

One-in-eight women in the United States are diagnosed with breast cancer in their lifetime. Epidemiologic studies, and rodent models, show that moderate-to-vigorous intensity physical activity (MVPA) decreases the risk of breast cancer. Proposed mechanisms of how physical activity impacts breast cancer initiation and progression range from minimizing risk factors to reducing proliferation and increasing apoptosis of mammary cancer cells. Myokines are muscle-derived cytokines excreted by skeletal muscle following acute exercise. Specifically, the myokine oncostatin M (OSM), has been shown to decrease breast cancer cell proliferation, *in vitro*. We hypothesized that OSM is involved in physical activity-induced breast cancer prevention, *in vivo*. Female Sprague Dawley rats were injected with 50 mg/kg n-methyl-n-nitrosourea (MNU) at 22 days of age to induce mammary adenocarcinoma. Rats were exercise trained (EX) or remained sedentary in standard cage conditions (SED). Additional groups were treated with anti-OSM antibody (SED+Anti-OSM and EX+Anti-OSM) to explore the impact of OSM blockade. The study was powered with n=12 per group to observe a significant difference in tumor free survival time across four groups. Comparisons were made regarding tumor latency, relative tumor latency, baseline OSM levels, and OSM levels after an acute exercise test (AET). Exercise training consisted of treadmill acclimation, and progressive increases in session duration, speed, and grade, until reaching 30 min/day, 20 m/min at 15% incline. Exercise training continued 5 days/week until tumor palpation reached 4cm^3 or week 19, which ever came first. Rats completed an AET at that time. Blood was collected in a time course (before, immediately following, and 2hr following AET) to determine OSM plasma levels. We observed no significant differences between growth curves of rat body weight over the course of the intervention. Relative tumor free survival time was significantly longer in EX animals (1.36±0.39) compared to cohort control SED animals (1.00±0.17; $p=0.009$, $p<0.05$), SED+Anti-OSM animals (0.90±0.23; $p=0.019$), and EX+Anti-OSM

animals (0.93±0.74; p=0.004). There were no significant differences between SED, SED+Anti-OSM, or EX+Anti-OSM animals. An interaction between anti-OSM and EX was observed with marginal significance (p=0.08) after a 2-way ANOVA analysis. Following AET, OSM plasma levels were higher compared to baseline OSM levels, but not statistically significant in non-tumor bearing adult rats. There were no significant differences in OSM plasma levels after acute exercise test when comparing tumor bearing SED and EX animals. However, there was evidence that tumor size and changes in OSM plasma concentration after AET were negatively correlated (r=-0.72; p=0.001). In conclusion, we observed that exercise-induced delay of mammary tumor development was mitigated through anti-OSM administration. While breast cancer tumor free survival time may be modulated by exercise-induced increases of circulating OSM, our results also show that tumor burden may impact OSM release from muscle. Further exploration regarding this correlation would help improve identification of potential therapeutic targets. Thus, future studies of the OSM mechanism will lay groundwork for developing novel chemo-prevention strategies in women who are unable or unwilling to exercise.

TABLE OF CONTENTS

LIST OF FIGURES

LIST OF TABLES

LIST OF ABBREVIATIONS

AET	Acute Exercise Test
Anti-OSM	Oncostatin M Antibody
BDNF	Brain-Derived Neurotrophic Factor
C/EBPδ	CCAAT/Enhance-Binding Protein Delta
CO2	Carbon Dioxide
ELISA	Enzyme-Linked Immunoassay
ER	Estrogen Receptor
EtOH	Ethanol
EX	Exercise animals
FGF	Fibroblast Growth Factor
GDF5	Growth Differentiation Factor 5
gp130	Glycoprotein130
HER2	Her-2/Neu
IL	Interleukin
IP	Intraperitoneally
JAK	Janus Kinase
kg	Kilogram
LIF	Leukemia Inhibitory Factor
MaxET	Maximal Exercise Test
μg	Microgram
mg	Milligram
mL	Milliliter
MNU	n-Methyl-n-Nitrosourea

MRI	Magnetic Resonance Imaging
MSOT	Multispectral Optoacoustic Tomography
MVPA	Moderate-to-Vigorous Intensity Physical Activity
NaOH	Sodium Hydroxide
NBF	Neutral Buffered Formalin
OSM	Oncostatin M
PBS	Phosphate-Buffered Saline
PR	Progesterone Receptor
SED	Sedentary animals
STAT3	Signal Transduction and Activator of Transcription-3
TV	Tumor Volume
TTV	Total Tumor Volume
Type I OSM-R	OSM Type I Receptor
Type II OSM-R	OSM Type II Receptor
wpi	Weeks post-injection

ACKNOWLEDGEMENTS

Thank you to my research team who played an integral part in helping me complete my Masters project: Katie Wehreng, Dhruvil Shah, Dan Lin, Hongke Wu, and Dr. Kathleen Sturgeon. I would not have been able balance my research timeline and residency responsibilities without you all. Thank you to my committee for the collaboration and reviews of my thesis: Dr. Kathleen Sturgeon, Dr. Tiffany Whitcomb, Dr. Henry Thompson, and Dr. Jenelle Izer.

An additional special thank you goes out to everyone who supported me throughout this research and residency: my family, Clover, the Department of Comparative Medicine faculty and staff, and my resident mates: Dr. Caroline Chang, Dr. Rachel Griffin, Dr. Genesis Newton, Dr. Lori Sampsell, and Dr. Ashley Varley.

I would like to acknowledge the following groups that helped with extensions of this thesis: The Pennsylvania State University College of Medicine Molecular and Histopathology Core, the ONE Group research team, the Biophotonics and Ultrasound Imaging Laboratory at University Park, and BioRender.com.

We would also like to thank the funding that made this work possible: Department of Comparative Medicine and Department of Public Health Sciences at The Pennsylvania University College of Medicine.

Chapter 1

INTRODUCTION

1. Breast Cancer Overview

Breast cancer is the second leading cause of female cancer-related death, worldwide.[1] One-in-eight women within the United States will develop breast cancer in her lifetime.[1] Accounting for 30% of new cancer diagnoses, breast cancer is the most common malignant neoplasm in women.[2,3] Women are 100 times more likely to develop breast cancer compared to men.[3] Despite increased identification and awareness of modifiable risk factors, the incidence of breast cancer is rising and expected to continue to increase (64% from 2011 to 2030).[2,4]

There is a wide range of risk factors associated with breast cancer. Aside from sex, the most significant risk factors include age, family history and genetics, estrogen exposure, reproductive status, and lifestyle risks.[5] Family history poses a significant risk due to inheritable genetic mutations (e.g. *BRCA1, BRCA2, TP53, PTEN, PALB2,* etc) in genes or epigenetic modifications.[4-6] Estrogen exposure, both endogenous and exogenous, may increase a women's risk for breast cancer.[5] Late menopause and early menarche have both been shown to increase the likelihood of breast cancer development.[3,5,7] The three most common lifestyle risks reported are smoking, obesity and alcohol consumption.[3,5]

Although the incidence of breast cancer is rising, early identification and intervention has allowed for improved prognoses.[5] Early intervention relies on regular mammography screenings, especially in high-risk patients.[3] Once detected, pathologic examination and diagnostic imaging can help guide treatment options. Common immunohistochemical markers used in routine pathology of tumor tissue include estrogen receptor (ER), progesterone receptor (PR), and Her-

2/neu (HER2). The presence or absence of these markers predict responses to treatment. Additional staging through mammography or MRI may be performed to identify local involvement of the lymph nodes, while radiographs and blood work should be used to identify metastatic involvement.[8]

The economic burden of breast cancer is substantial with the highest treatment costs compared to all cancers. It was estimated, in 2020, that the cost for medical services related to breast cancer was $26.2 billion within the United States.[9] Surgical intervention remains the most commonly utilized treatment for local and regional involvement. Patients at high risk for reoccurrence also may undergo chemotherapy or other adjunctive treatments based on receptor presence on histopathology, tumor size, and lymph node involvement. Radiation in combination with surgical removal has been used for early-stage breast cancer successfully.[8] Mortality rates have decreased over time due to improved diagnostics and treatments at early stages of the disease. Further research is being done regarding minimizing risk factors prior to breast cancer development.[3,5]

1.1. Breast Cancer Prevention

Several preventative measures are currently utilized to minimize the risk of breast cancer for moderate and high-risk women. There are various surgical approaches that can be performed for those with known familial risks. Additionally, some pre-menopausal women at elevated risk for breast cancer may opt for estrogen reduction strategies such as bilateral salpingo-oophrectomy, or pharmacological intervention.[3] Women that do not have genetic or family history risk factors may choose to focus their prevention efforts on lifestyle modifications. Quitting smoking, weight loss in post-menopausal women with excess weight, increased physical activity, and limiting alcohol use are associated with decreased risk of breast cancer.[3,5]

1.1.1. Physical Activity as Breast Cancer Prevention

Research involving physical activity as a cancer prevention method has become increasingly popular since the early 2000s.[10] A review article by Ballard-Barbash *et al* describes current research involving physical activity and breast cancer. The strongest evidence supporting physical activity as a risk reduction strategy is associated with pre-diagnosis activity.[10] There is also convincing epidemiologic evidence that higher intensity physical activity level is associated with a 10-25% lower risk of breast cancer, compared to inactivity.[11,12]

The mechanism behind the impact of physical activity on cancer risk factors may involve several different pathways and impact all stages of carcinogenesis (initiation, promotion, and progression).[2,6] Exercise may reduce cancer risk indirectly by contributing to the maintenance of a healthy body weight, or through biologic pathways.[2,13] For instance, exercise training promotes anti-oxidant defenses. Therefore, oxidative microenvironments associated with tumors are targeted after exercise. This effect is beneficial for decreased risk of both initiation and progression of cancer.[14]

Furthermore, biologic mechanisms related to breast cancer prevention may involve altering local microenvironments, the malignant transformation processes (decreasing cell proliferation and increasing apoptosis), or cancer metabolism.[2,15] Systemic factors that have been identified to modulate such biologic processes include, but are not limited to inflammation, reduced adiposity, and myokines.[6,16,17] Overall systemic inflammation is shown to increase risk of cancer. Physical activity promotes anti-inflammatory processes that, in turn, prevent cancer through altering the tumor microenvironment.[16]

Altered cancer metabolism through reduction of adiposity has several potential mechanisms of reducing breast cancer risk in post-menopausal women.[16] Incidence and recurrence of breast cancer is associated with increased insulin levels.[2,16,18] These patients are also at risk of

comorbidities like type 2 diabetes. Physically active patients may have improved prognosis through reduction of such comorbidities.[14,16] Additionally, in post-menopausal women, circulating estrogen primarily originates from adipose tissue.[18] Endogenous estrogen associated with delayed menopause is a known risk factor for breast cancer; therefore, by reducing adiposity, estrogen exposure risks are lessened.[18]

Of particular interest to this study, the role of myokine release by skeletal muscle in inhibiting cancer cell proliferation and inducing apoptosis are currently being explored.[13,15] See Figure 1-1 for a summary of some pathways being explored involving physical activity induced cancer prevention.

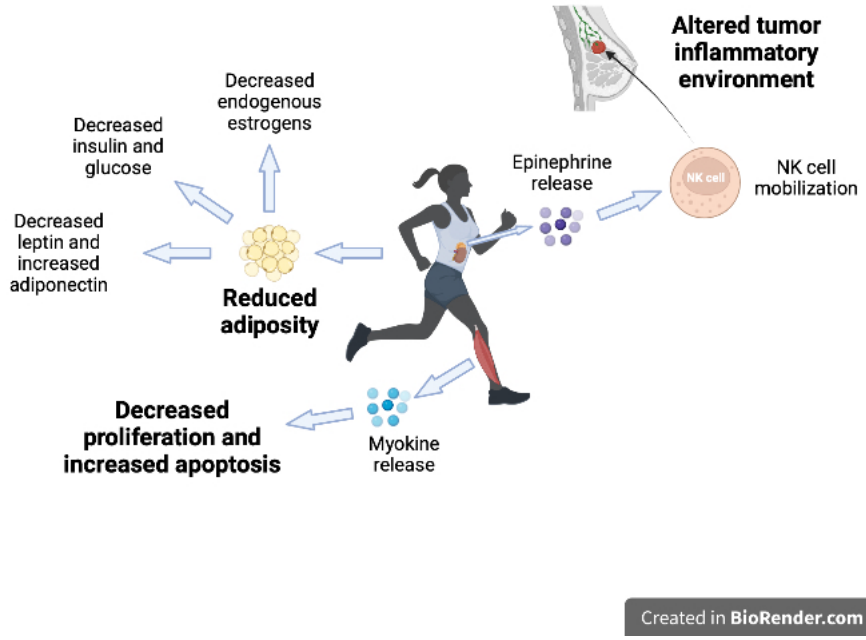

Figure **1-1**: Selected pathways of cancer prevention by physical activity discussed in this thesis. Physical activity decreases risk factors by reducing adiposity, altering tumor microenvironment, and decreasing cancer cell proliferation and increased cell apoptosis.

1.2. Myokines

Muscle-derived cytokines, or myokines, are peptides that are released by skeletal muscle during exercise.[19] Each myokine responds to different levels of activity and functions differently within the body. Myokines may have autocrine or endocrine effects. Moreover, myokines with endocrine effects may cause physiologic and metabolic adaptations in other organs.[19,20]

Currently explored myokines include, but are not limited to: myostatin, fibroblast growth factor (FGF), interleukins (IL-6, IL-7, IL-8, IL-15), leukemia inhibitory factor (LIF), oncostatin M (OSM), and brain-derived neurotrophic factor (BDNF).[20,21] IL-6 is a cytokine that was originally discovered as a myokine with both paracrine effects on the muscle and endocrine effects throughout the body.[19] It elevates in response to acute exercise episodes. However, there is also evidence that exercise training programs decrease the overall circulation of IL-6.[22] Increased fat metabolism is a primary effect of exercise-induced IL-6 release; this has been shown both *in vitro* and *in vivo*.[19,22] On the other hand, some myokines, including FGF-21 and irisin, increase in response to endurance programs.[19,20] Both FGF-21 and irisin also play roles in obesity management through increasing lipolysis.[19]

Endocrine effects of myokines extend beyond the effect on adipose tissue after exercise. For example, BDNF release by the hippocampus after exercise has positive impacts on cognitive function, such as learning and memory.[19] Recent literature has shown that BDNF release is regulated by other myokines including irisin and FGF-21.[19,22] IL-6 also has a systemic anti-inflammatory effect after exercise. This pathway is controlled through cortisol production by the adrenal gland and circulating macrophages.[22]

1.2.1. Oncostatin-M (OSM)

OSM is myokine that is a part of the IL-6 cytokine family with IL-6, LIF, and ciliary neurotrophic factor.[23] These cytokines are classified together due to sharing a common signaling receptor subunit, glycoprotein 130 (gp 130).[24] OSM can act through an OSM Type I Receptor (Type I OSM-R) or OSM Type II Receptor (Type II OSM-R), with both receptors containing the gp130 subunit. Type I OSM-R contains a LIF receptor subunit, and Type II OSM-R contains an OSM-R specific subunit, OSMRβ.[24,25]

Many roles of OSM have been explored in both normal physiology as well as disease states.[21] Immunity, hematopoiesis, homeostasis, and development are some pathways that have been studied.[26] The role of OSM in increasing cell apoptosis and decreasing cell proliferation in normal mammary tissue during development depends on binding to the Type II OSM-R, specifically.[23] This interaction activates the Janus Kinase family (JAK) signaling pathway that further activates the Signal Transduction and Activator of Transcription-3 (STAT3) protein.[23,27] Downstream cascades lead to increased cell apoptosis and decreased proliferation after transcription of CCAAT/enhance-binding protein delta (C/EBPδ) within the nucleus. C/EBPδ is responsible for decreasing cellular growth by limiting cells in the S-phase and increasing expression of cells in G_0 phase of the cell cycle.[23] See Figure 1-2 for a visual representation of the OSM pathway.

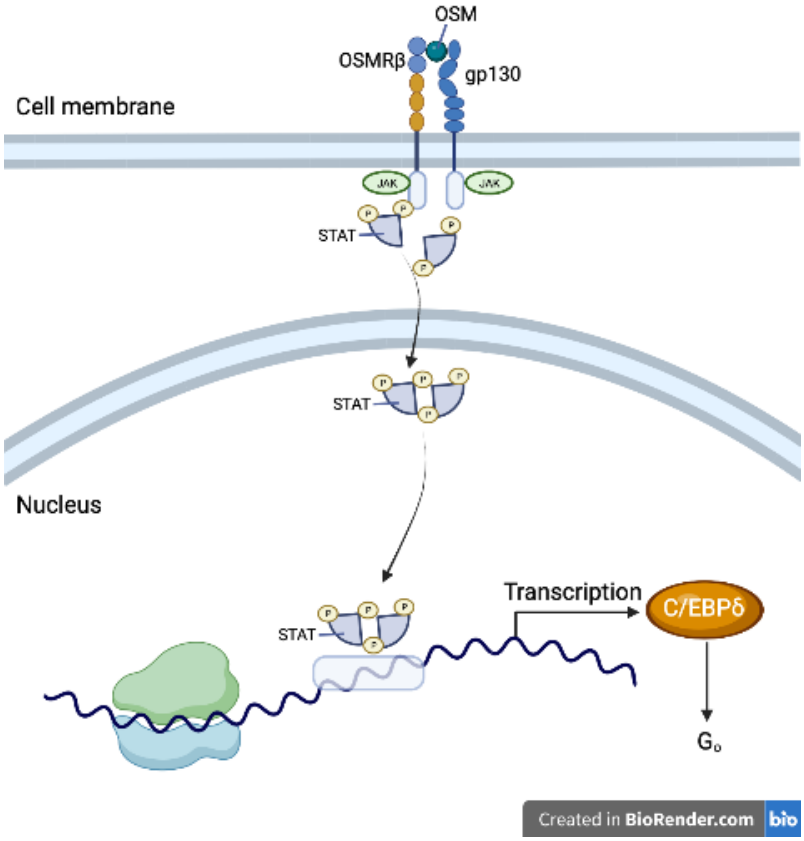

Figure **1-2**: OSM binding to the OSMRβ receptor triggers the STAT3 pathway leading to cell arrest by C/EBPδ.

Studies have shown that OSM levels increase in systemic circulation following exercise.[28] An acute exercise bout increases serum OSM 3-fold compared to baseline levels in a mouse model after a 60-minute forced-swim test.[29] The pulsatile action of OSM returned to baseline concentrations after two hours. This study also showed that there was increased expression of OSM in the anterior tibialis, gastrocnemius, and soleus muscles following exercise.[29] This increase in serum OSM was similarly observed in both younger and older male humans after cycling.[30] A recent study in obese humans showed that OSM had increased plasma circulation following a 30-minute exercise episode, and was stable when comparing before and after an 8-week endurance training.[31]

In regard to cancer, OSM has been noted to have differing impacts on several tumor types. OSM has an inhibitory effect on cancers such as melanoma, lung, and breast cancer.[25] Decreased cell proliferation appears to be the primary mechanism of inhibition.[26] Hojman *et al*, showed that human breast cancer cells (MCF-7) cultured with OSM-rich serum had significantly decreased cell proliferation compared to cells with control serum.[29] However, there is contradictory research that supports synergistic effects of OSM with tumor development, tumor progression, and metastasis in some cancers.[26,32,33]There is evidence of OSM overexpression in colon cancer, pancreatic cancer, myeloma, and brain tumors.[34] A feed-forward loop of OSM-R triggered STAT3 may also promote tumorigenesis in cancers such as glioblastoma or cervical cancer.[26,34,35] In breast cancer specifically, Araujo *et al* showed that presence of OSM and OSM-R in the tumor microenvironment promotes cancer progression.[32]

Although research regarding OSM and breast cancer has differing results, there are few *in vivo* studies regarding the impact of OSM peptide blockade on breast cancer specifically. Research in this area will have an important impact because it could lay the groundwork to develop novel prevention strategies in human patients. Molecular pathways that are modulated by exercise may provide drug-able targets for breast cancer patients who ultimately cannot, or will not, take part in exercise programming as part of their clinical care.

2. Specific Aims

The overall goal of the proposed study was to elucidate the role of OSM in exercise-induced decreased breast cancer risk by leveraging an animal model of mammary carcinoma. We examined this through experiments divided into three aims. All experiments were performed using young, female Sprague Dawley rats with chemically induced mammary neoplasia by N-methyl-N-nitrosourea (MNU) injection.

Aim #1: Ascertain the magnitude of exercise-induced delayed latency of breast cancer in our carcinogenic rat model. We hypothesized that rats under standard cage conditions will develop mammary tumors at a faster rate compared to exercise trained rats.

Aim #2: Identify the impact of OSM blockade on exercise-induced delayed latency. First, the appropriate dose and frequency of OSM antibody (anti-OSM) administration was selected through a pilot study. We hypothesized that OSM blockade concomitant to exercise training would mitigate delayed latency compared to exercise trained animals. We also hypothesized that OSM blockade would accelerate tumor onset in sedentary animals compared to sedentary animals without blockade.

Aim #3: Determine the impact of exercise training on OSM plasma levels. A blood draw time course was conducted prior to and following a single acute exercise episode. We hypothesized first that baseline levels of OSM in exercise trained animals would be higher than baseline levels in sedentary animals. We also hypothesized that plasma levels of OSM after acute exercise would have a greater magnitude of change in rats that underwent exercise training.

Chapter 2

MATERIALS AND METHODS

1. Animals

Female Sprague Dawley rats (NTac:SD; *Rattus norvegicus*) were purchased from Taconic Biosciences, Inc. (Germantown, NY, USA) at 17 to 28 days of age. Nine rats were received at 28-days of age for use in a pilot study to provide proof of concept for delayed latency of breast cancer during exercise training. Six rats were received at 24-days old for use in a pilot study to determine anti-OSM dose and safety. Forty-eight 17-day old rats were received for the remainder of experiments. When rats were received at 17-days old, a retired breeder female was sent with the litter. Retired female breeder rats (LACT; n=3) were used separately for acute exercise experiments as size matched (250-275g), sedentary animals without MNU injection or exercise intervention.

All rats were acclimated to the facility for three days prior to manipulation. Rats were group housed in conventional caging on corncob bedding (Teklad Corncob 7097, Inotiv, West Lafayette, IN, USA). All rats had *ad libitum* access to food (Teklad Global Diet 2018, Inotiv, West Lafayette, IN, USA) and filtered water via automatic watering system. The housing room had a 12:12 hour light:dark cycle. The room was maintained with constant temperature (72±2^{o}F) and humidity between 30 to 70%. All rats were determined pathogen free from: *Clostridium piliforme, Filobacterium rodentium, Mycoplasma pulmonis, Pneumocystis* spp., Kilham Rat Virus, Rat Theilovirus, Pneumonia Virus of Mice, Rat Coronavirus, Sialodacryoadentitis Virus, Rat Minute Virus, Rat Parvovirus, Toolan's H1 Virus, Hantaan Virus, Lymphocytic Choriomeningitis Virus, Mouse Adenovirus I and II, Reovirus 3, Sendai Virus, ectoparasites, and enteric helminths through dirty-bedding transfer to sentinel animals. Sentinel rats were collected at the conclusion of each cohort of animals. All procedures were performed at an AAALAC-International accredited facility

with approval by The Pennsylvania State University College of Medicine Institutional Animal Care and Use Committee in accordance with the *Guide for the Care and Use of Laboratory Animals*.[36]

2. Pilot Studies

Two pilot studies were conducted in order to: 1) determine MNU dose and administration timing, 2) select appropriate acute exercise testing parameters (duration, speed, incline), and 3) determine anti-OSM dose and safety for this study.

2.1. MNU Pilot

Ten female Sprague Dawley rats were received at 28-days of age and allowed to acclimate to the facility before experimental manipulation. At 35-days of age, all ten rats received a single injection of 75 mg/kg MNU (Tyger Scientific Inc., Ewing Township, NJ, USA), intraperitoneally (IP). Rats were divided into two groups: sedentary (SED; n=5) or exercise trained (EX; n=5). Two rats were removed from the study for a resulting experimental group count of SED n=4 and EX n=4. One rat was removed from the study due to unexpected death during restraint for venipuncture. The second rat was removed from the study due to refusing to run.

Rats were acclimated to the motorized treadmill (Panlab Touchscreen Treadmill, Harvard Apparatus, Holliston, MA, USA) for three days prior to exercise training. The rats were allowed to explore the treadmill without turning on the belt for 10 minutes on the first day of acclimation. On day 2 of acclimation, the treadmill belt speed was increased to 5 m/min at 0% incline. On day 3 of acclimation, the treadmill belt speed was increased to 10 m/min at 0% incline. Prior to starting the treadmill belt on days 2 and 3 of acclimation, the rats were allowed to sit on the stationary treadmill for 5 minutes.

After acclimation, all rats underwent an initial maximal exercise test (MaxET; Table 2-1). Speeds of the treadmill were quickly increased at increments of 5 m/min until the rat could no longer keep up with the speed of the treadmill. Rats ran at the final speed until they refused to run. Refusal to run was defined as a rat sing on the shock grid for 30 consecutive seconds at 0.4 mA intensity without returning to the treadmill belt. Serial blood samples were collected before, immediately after, and 2 hours after the MaxET via tail vein. Plasma isolated from the blood was evaluated using the Rat Oncostatin M ELISA Kit from Novus Biologicals (Centennial, CO, USA).

Table **2-1**: Maximal exercise test protocol on motorized treadmill increased speeds rapidly and reached higher speeds compared to daily exercise training.

SPEED (m/min)	GRADE (%)	DURATION (min)
25	10	3
40	10	3
45	10	1
50	10	1
55	10	1
60	10	1

Exercise training began following the initial MaxET with two weeks of gradual increases in the treadmill speed, incline, and session duration until rats reached a maximum speed of 20 m/min, 15% incline, for 30 min/day. Rats were exercised for 5 days/week. See Treadmill Protocols, Table 2-2 (Section 3.1.2), for exercise training protocol details. During all exercise training

episodes, SED rats were exposed to the vibrations and noises of the treadmill by placing them on the same table within their home cage. Exercise conditions were continued until study completion.

Mammary chains of each rat were palpated twice per week for detection of tumors. Tumors were measured twice per week with digital calipers until tumors reached total volume (TTV) of $4cm^3$ or 18 weeks post-MNU injection, whichever came first. After TTV reached $4cm^3$ or 18-weeks post-MNU injection, all rats underwent a second MaxET. Humane endpoints were selected to allow for early euthanasia if the size or location of the tumor interrupted normal ambulation, weight loss exceeded 20%, or if a rat was moribund. During this pilot, no rats were euthanized due to reaching a humane endpoint.

All rats were euthanized within 48 hours after the second MaxET by inhalation of CO_2 followed by exsanguination and tissue collection. Mammary tumor weight, heart weight, and carcass weight were recorded at the time of necropsy. Tissues collected for additional analysis in this study included: plasma, mammary tumor, and mammary chain (contralateral to tumor). Other tissues banked for future studies included: anterior tibialis muscle, gastrocnemius muscle, soleus muscle, hind limbs, heart, and lung.

Following our observations in this pilot (Chapter 3, Section 1), adjustments in the age of the rats and dose of MNU were implemented for the final experiment to alter timing of tumor onset. Additional changes to the final experiment were made to address the lack of measurable changes in OSM plasma concentrations after the MaxET in all animals tested. The MaxET parameters were adjusted for speed and duration of the treadmill session to increase OSM response. The final experiment also removed the initial exercise test because the rats were too small to obtain adequate blood samples for the ELISA.

Parameters for the new acute exercise test (AET) were piloted using SED non-tumor bearing rats (n=4) that were set to be randomized into the anti-OSM trial. Section 3.1.3. describes

the AET protocol. Future cohorts of animals underwent a single AET after tumor palpation and growth, as described in the final experiment (Section 3).

2.2. Anti-OSM Pilot

An additional six, 24-day old rats were received for an anti-OSM pilot to determine dose and safety of the Mouse Oncostatin M/OSM Antibody (R&D Systems Inc, Minneapolis, MN, USA). Anti-OSM was reconstituted per manufacturer's recommendations as described in Section 5. Doses for the anti-OSM pilot were initially chosen based on neutralizing levels of anti-OSM, *in vitro*, as listed on the manufacturer's website, due to lack of an available rat OSM antibody and lack of publications regarding dosing.

First, rats were divided into low dose (0.18 μg/rat; n=3) and high dose groups (0.9 μg/rat; n=3). Each rat was injected with anti-OSM once, IP. Blood sampling was repeated once a week for three weeks beginning 24 hours after the injection. Plasma was isolated from blood for OSM concentration analysis using ELISA.

Due to lack of measurable change in OSM plasma concentrations after anti-OSM injection during this pilot, the same rats underwent an additional trial after a one-month wash out period. This was performed to determine safety and efficacy of higher doses. Rats were divided into groups based on frequency of injection: once weekly (1.8 μg/rat; n=3) or twice weekly (1.8 μg/rat; n=3). Blood collection was repeated once a week for three weeks, beginning 24-hours post-injection. Plasma was isolated from blood as previously described for OSM concentration analysis using ELISA.

Further difficulties with measurable changes in OSM plasma concentration after anti-OSM injection led to adjustments in dose and timing of anti-OSM. It was determined that the ELISA would not depict OSM decreases following OSM blockade by neutralizing antibody. We suspect

this was due to differences in epitopes for anti-OSM binding and ELISA detection of OSM protein. After dose extrapolation from mouse data, a dose of 50 μg/kg IP, once weekly, was selected for the final experiment.[37]

3. Experimental Design

Rats were received at 17-days of age and acclimated to the facility for 72-hrs. Figure 2-1 is a visual representation of the experimental timeline.

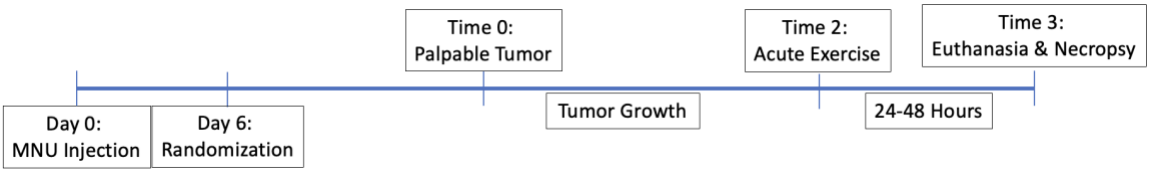

Figure **2-1**: Experimental Timeline

All rats were injected with 50 mg/kg IP MNU on Day 0 (22-days of age) and acclimated to the treadmill for three days. Rats were randomized into four experimental groups after MNU injection and their final day of acclimation to the treadmill (Day 6): SED (n=15), EX (n=15), SED+Anti-OSM (n=5), or EX+Anti-OSM (n=13). One rat was excluded from data analysis from the EX group because the rat refused to run, resulting in EX n=14.

Exercise training was continued during the light phase of the light cycle between Day 6 and Time 2, as depicted above, for rats in exercise training groups (EX and EX+Anti-OSM), thereafter (See Section 3.1 for exercise training protocols). During all exercise training episodes, SED and SED+Anti-OSM rats were exposed to the vibrations and noises of the treadmill by placing them on the same table within their home cage. Rats in the SED+Anti-OSM and EX+Anti-OSM groups were injected IP with anti-OSM at 50 μg/kg once per week.

Rat mammary chains were palpated three times weekly for detection of tumors. Once palpable, all tumors were measured with digital calipers three times weekly to obtain a calculated tumor volume. The formula below describes tumor volume (TV) calculation where "a" represents the tumor length (cranial to caudal measurement) and "b" represents the tumor width (medial to lateral measurement) (See Figure 2-2 for visual representation of measurements).[38] If rats had multiple tumors, TTV was calculated by adding the calculated volumes of each tumor together.

$$TV = \frac{b^2 \times a}{2}$$

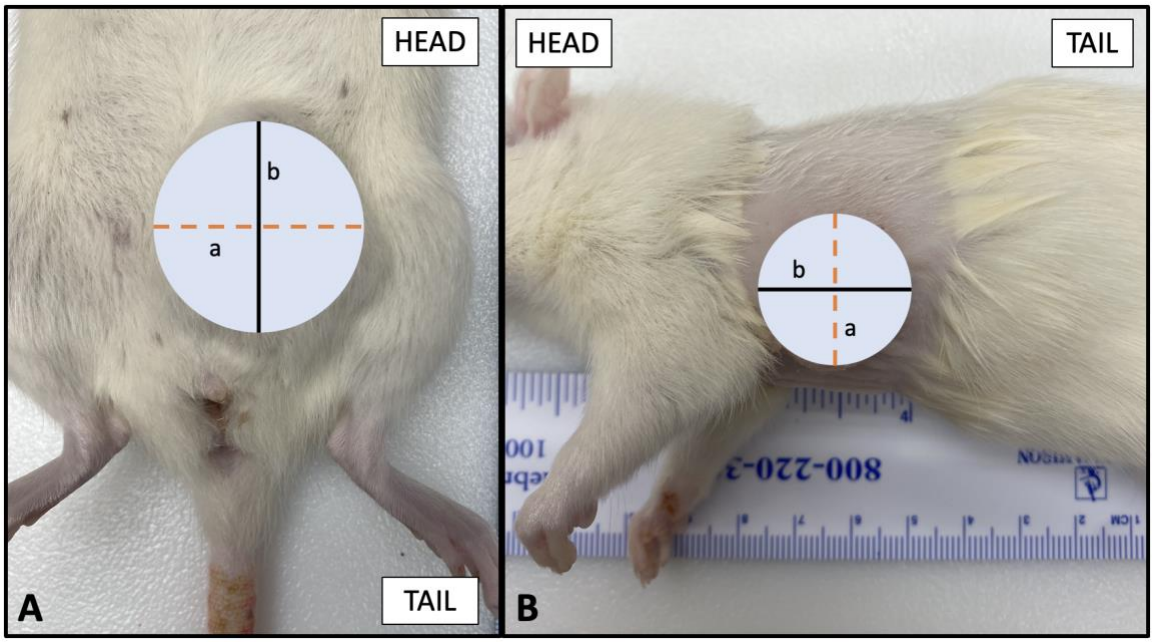

Figure **2-2**: Visual representation of tumor measurements. A) Tumor measurements for an inguinal tumor with the rat laying in dorsal recumbency. B) Tumor measurements for an axillary tumor with the rat laying in lateral recumbency. Dashed orange line represents the width (b) measurement and solid black line depicts the length (a) measurement.

Once a single tumor reached 1.5-2.0 cm^3, select rats were used in an unrelated study using non-invasive, photoacoustic imaging by multispectral optoacoustic tomography (n=5; MSOT inVision, iTheraMedical, Munich, Germany) or Acoustic X (n=18; Cyberdyne Inc, Tsukuba, Japan). Rats were sedated for imaging with a single IP injection of 80 mg/kg ketamine (AuroMedics

Pharma LLC, East Windsor, NJ, USA) and 8mg/kg xylazine (AnaSed®, Akorn Operating Company LLC, Gurnee, IL, USA). Results of imaging are not described in this thesis.

Rats were allowed to recover after sedation for 24 hours prior to returning to exercise training, if in an exercise group. Exercise training resumed until TTV reached $4cm^3$ (Time 2). After TTV reached $4cm^3$, rats underwent an AET. Alternatively, if the rat did not develop a tumor by week 19 post-injection, or the TTV did not reach $3cm^3$ by week 5 post-palpation, the rat underwent an AET at that time. Serial blood samples were collected from all rats via tail vein before, immediately after, and 2-hours post-acute exercise. Plasma was isolated from blood for ELISA to determine plasma OSM concentration.

Rats were excluded from the AET population after involvement in the photoacoustic imaging study or if the rat refused to run. Three rats experienced acute death secondary to complications with MSOT (drowning) or Acoustic X (anesthetic complication), thus an AET was not possible. Experimental groups for AET were divided into non-tumor bearing SED (n=7), tumor bearing SED (n=4), tumor bearing EX (n=7), and tumor bearing EX+Anti-OSM (n=5).

Rats were euthanized early for humane endpoints if the size or location of the tumor interrupted normal ambulation, weight loss exceeded 20%, or if animal was moribund. Within the final experiment, no rats were euthanized due to humane endpoint. All rats were euthanized 24 to 48 hours after AET (Time 3), by inhalation of CO2 followed by exsanguination and terminal tissue collection. Mammary tumor weights, heart weights, and carcass weights were recorded at the time of necropsy. Additional tissues collected included: plasma, mammary tumor, anterior tibialis muscle, gastrocnemius muscle, soleus muscle, hind limbs, heart, and lung. Tissues were divided between frozen and fixed samples based on future use.

3.1. Treadmill Protocols

Figure 2-3 shows a labeled diagram of the motorized treadmill (Panlab Touchscreen Treadmill, Harvard Apparatus, Holliston, MA, USA) used in this study.

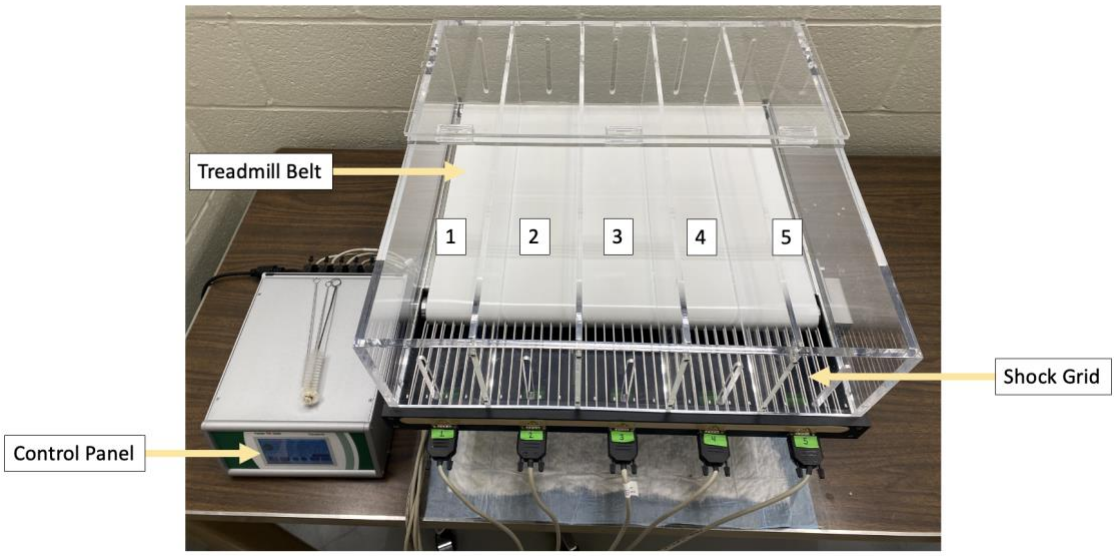

Figure **2-3**: Labeled diagram of motorized treadmill. Numbers indicate the lane number.

3.1.1. Acclimation

All rats were acclimated to the motorized treadmill over three days. On day 1 of acclimation, rats were placed on a stationary treadmill for 45 minutes. Day 2 of acclimation allowed the rats to sit on a stationary treadmill for 15 minutes, followed by 5 minutes of movement at 5 m/min at 0% incline. Day 3 of acclimation included 15 minutes of stationary treadmill, followed by 5 minutes at 10 m/min at 0% incline. Cheerios were used for positive reinforcement at the opposite end of the treadmill from the shock grid for all days of acclimation. The shock grid was not activated during acclimation. Rats were gently tapped on their tail base with a soft brush if they sat on the shock grid for more than 1 sec without self-correction during days 2 and 3 of acclimation.

3.1.2. Exercise Training

All exercise trained rats underwent a two week ramp up to reach maximum training at 20 m/min, 15% incline, 30 min/day. Rats were exercised five days per week. Table 2-2, below, outlines the ramp up and exercise training protocol. All exercise sessions involved a 2–3-minute warm-up and cool-down period immediately before and after the exercise session, respectively.

Table **2-2**: Motorized treadmill exercise training protocol.

WEEK	DAY	SPEED (M/MIN)	GRADE (%)	DURATION (MIN)
1	1	15	0	10
	2	17.5	0	15
	3	20	0	20
	4	20	5	25
	5	20	5	30
2	1	20	10	30
	2	20	10	30
	3	20	10	30
	4	20	15	30
	5	20	15	30
3-6+	1-5	20	15	30

3.1.3. Acute Exercise Test (AET)

Rats in all groups underwent an AET after TTV reached 4cm^3. The AET involved a 2-minute warm up period to reach 20 m/min speed. The session lasted for 60 minutes at 0% incline. A 2-minute cool down was allowed prior to serial blood collection as described previously.

3.1.4. Rat Compliance Protocol

After acclimation, rats were encouraged to run via positive reinforcement. Cheerios were given on a stationary treadmill at the opposite end of the shock grid before and after all training sessions. If rats stopped running for more than 1 second (e.g. sit on shock grid without self-correction), a soft brush was tapped on their tail base. If there was no response to the brush, or if the rat was distracted by the brush, the brush would be removed from the treadmill. The edge of the brush would then be used to make a sound on the exterior of the acrylic lane divider.

The shock grid was turned on at 0.2-0.4 mA if the rat did not self-correct within 3 seconds after either tapping or noise. Additionally, the shock grid was turned on if the rat was repeatedly non-compliant for a total of more than 5 seconds at a time. Rats would be removed (i.e. shock grid would be turned off, and the rat would not be encouraged to run) from a treadmill session if the rat stopped responding to the shock grid or if the total time spent off the treadmill was greater than 20% of the total running time (e.g. 6 minutes). Two rats were excluded from analysis due to lack of running.

4. N-methyl-n-nitrosourea (MNU)

MNU was stabilized by the manufacturer in acetic acid prior to shipment and stored in a single use vial with a rubber stopper at 4^{o}C, protected from light. All MNU was reconstituted in

0.9% NaCl at room temperature. After the addition of saline, the vial was gently agitated in a warm water bath at 37ºC until dissolved. All unused MNU was neutralized with 1N sodium hydroxide (NaOH) prior to disposal at a 1:1 volume ratio.

5. Anti-Oncostatin M Antibody (Anti-OSM)

Anti-OSM was stored at -20ºC if not reconstituted and diluted immediately after receipt. All Anti-OSM was reconstituted in 1X PBS at 7.4 pH at room temperature into a concentration of 33.3 μg/mL prior to injection. The sample was gently agitated by rocking for 10 minutes prior to use. Reconstituted samples were stored at 4ºC in between weekly injections for the duration of the study.

6. ELISA

Plasma OSM concentrations were measured using a Rat Oncostatin M ELISA kit per manufacturers guidelines. Blood was spun down at 10,000g for 15 minutes at 4ºC for plasma isolation. All plasma was placed directly on dry ice and frozen at -80ºC for long term storage. ELISA optimization was performed using plasma from control rats. Plasma was diluted 1:10, 1:20, 1:50, and 1:100 during optimization. It was determined to dilute all samples 1:10 with Standard/Sample Diluent prior to testing (optimization data not shown).

Analysis of the ELISA was completed using an SPECTRAMax M2 microplate reader (Molecular Devices LLC, San Jose, CA, USA) at 450 nm wavelength absorbance profile. SoftMax 5.0 (Molecular Devices LLC, San Jose, CA, USA) microplate reader program generated a 4-point quadratic standard curve for each ELISA run. The program used this standard curve to calculate

the final plasma concentrations for each sample. Each plasma sample was run in duplicate, where possible.

7. Mammary Immunohistochemistry

Mammary tumors and mammary chain contralateral to the tumor location were collected at the time of euthanasia. Sections were fixed in 10% Neutral Buffered Formalin (NBF) for five days prior to being switched to 70% ethanol (EtOH) for storage. Samples were paraffin embedded and stained for OSM-R protein (Rabbit Anti-Rat OSMR Antibody, MyBioSource.com, San Diego, CA, USA) by The Pennsylvania State University College of Medicine Molecular and Histopathology Core.

Images of tumors and mammary chains were collected using a Leica DM6 B microscope and camera with Leica Application Suite X (LAS X) imaging software (Leica Microsystems Inc, Deerfield IL, USA). Future analysis will compare OSM-R protein expression of both mammary chains and tumors in SED and EX animals.

8. Statistical Analyses

All statistical analyses were performed using SAS 9.4 (Cary, NC, USA). Unpaired t-tests assessed differences of latency and normalized latency between SED and EX groups. Latency and normalized latency comparisons were assessed across all experimental groups (SED, EX, SED+Anti-OSM, EX+Anti-OSM) using a one-way ANOVA with Bonferroni adjustment. A two-way ANOVA and Cohen's D were analyzed across all experimental groups to observe intervention interactions and effect size of anti-OSM. Unpaired t-tests were used to assess differences in baseline OSM concentrations in tumor bearing SED and EX rats. Unpaired t-tests were also used to compare

baseline OSM concentration to post-AET OSM concentration and post-AET OSM concentrations to 2hr post-AET OSM concentrations. Correlations between changes in plasma OSM and tumor size were performed using Pearson's correlation test. All statistical significance was assessed using a 2-sided P value < 0.05.

Chapter 3

RESULTS

1. MNU Pilot Results

Rat body weights were recorded weekly with Week 0 representing the rats' pre-MNU injection weight. Figure 3-1 below shows the rat body weight growth curves for SED and EX of the MNU Pilot. There were no significant differences in average body weight growth curves between experimental groups.

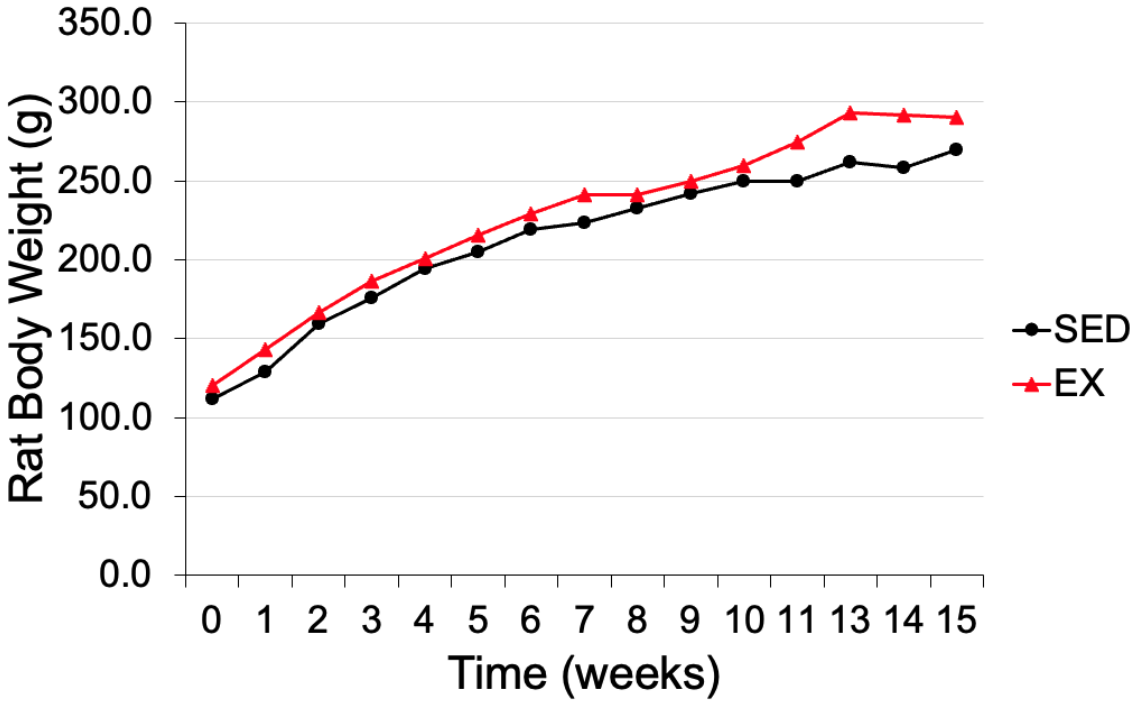

Figure **3-1**: Rat body weight growth curve over first 15 weeks of MNU Pilot. Week 0 = pre-MNU injection weight. No statistical significance. (SED n=4, EX n=5).

Heart weights were normalized to carcass weights for analysis. There was no significant difference noted between SED (0.0038 ± 0.0002) and EX rat (0.0039 ± 0.0004) heart-to-carcass weight ratio within the MNU pilot study. Figure 3-2 shows the average heart-to-carcass weight ratio of both groups in the MNU pilot study.

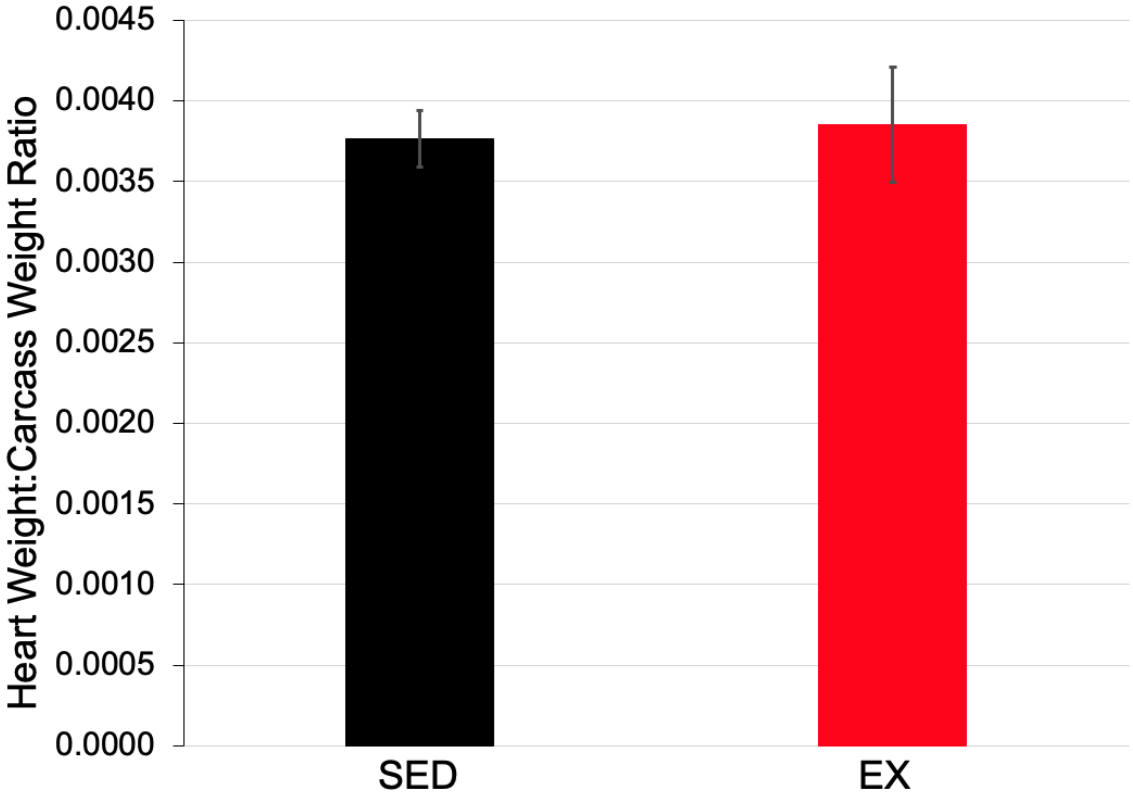

Figure **3-2**: Average heart weight to carcass weight ratio between SED and EX groups. No statistical significance. (SED n=4, EX n=4).

One SED rat and one EX rat were excluded from latency analysis due to not developing tumors within the experimental timeline. Average tumor latency of SED rats was 10.2 ± 3.2 weeks post-MNU injection (wpi). This was not significantly longer than EX, however, it was trending towards significance with average tumor latency of EX rats at 14.7 ± 2.7 wpi (p=0.07). Figure 3-3 shows the average tumor latency between SED and EX groups in the MNU pilot study. The tumor latency survival curve shows a significantly different tumor free survival time between the two groups (p=0.025; Figure 3-4). Due to the length of time for tumor development being longer than expected (>12 weeks), the dose of MNU and age of the rat at injection were adjusted for the remainder of the study as described previously.

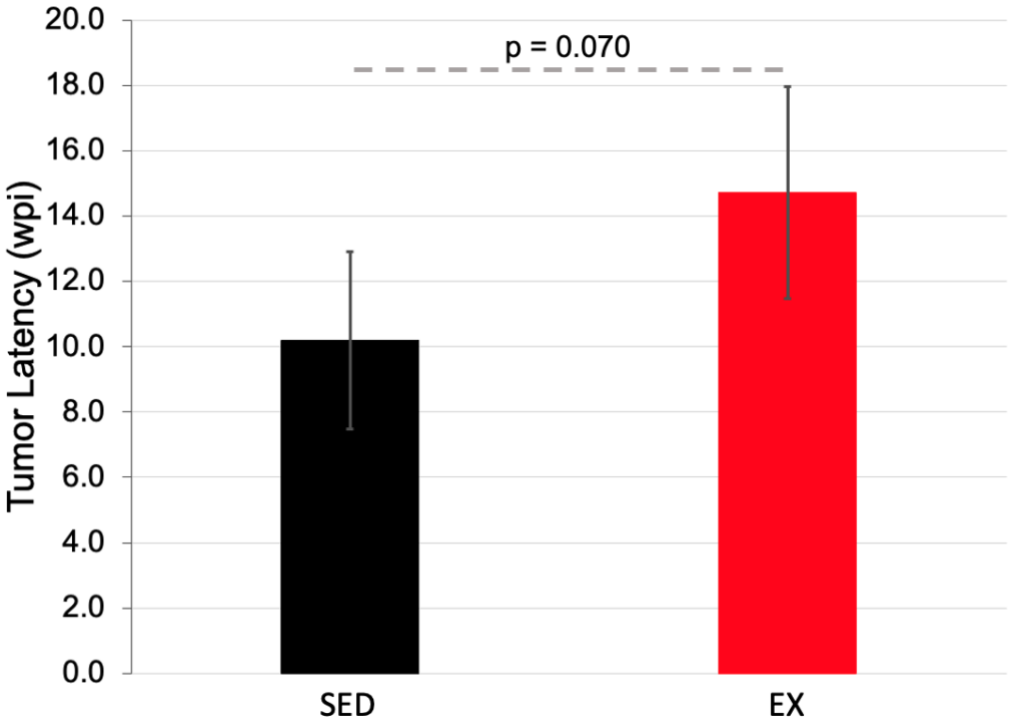

Figure **3-3**: Average tumor latency between SED and EX groups. Dashed bar indicates marginal significance. $p<0.05$. (SED n=3, EX n=3).

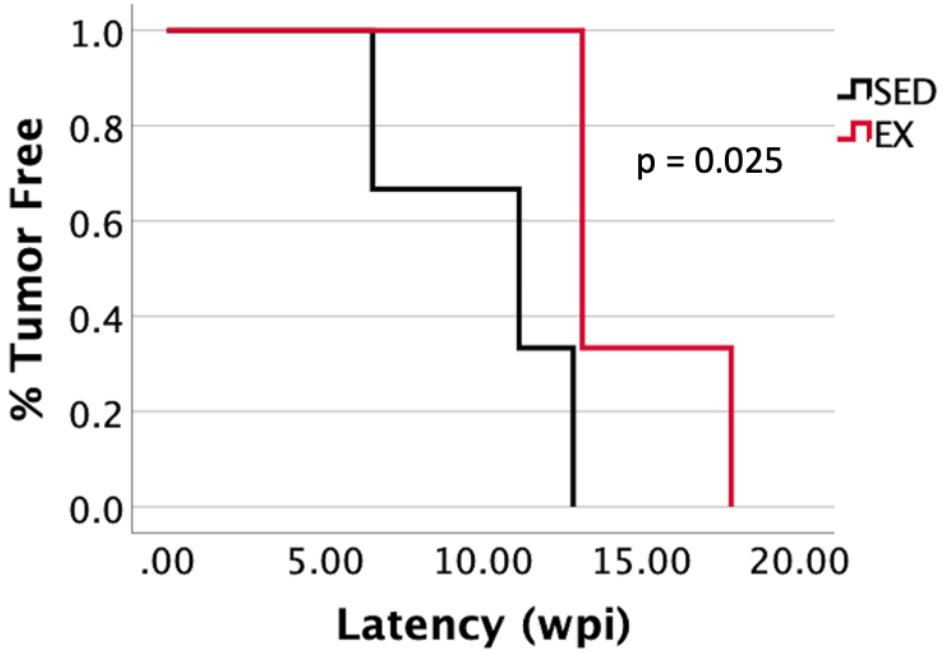

Figure **3-4**: Kaplan-Meier survival curve of percent tumor free survival for EX animals compared to SED animals. $p<0.05$. (SED n=3, EX n=3).

The other goal of the MNU pilot was to identify the appropriate acute exercise protocol to observe an increase in plasma OSM when comparing baseline OSM concentration and post-acute exercise OSM concentration. Initial MaxETs during this pilot were unsuccessful due to difficulty collecting adequate blood volumes for ELISA analysis. Additional MaxETs did not demonstrate an increase in OSM plasma concentration immediately after the exercise episode. Post-MaxET OSM plasma concentration was significantly lower than baseline levels ($p=0.030$, $p<0.05$). Figure 3-5 below shows that the average OSM concentration was lower immediately post exercise. Since there was no evidence of additional OSM release into the plasma after a MaxET with increasing speeds, all further tests were performed using the AET protocol (outlined in Chapter 2, Section 3.1.3). The AET double the amount of time rats spent on the treadmill compared to exercise training (60 min vs. 30 min), and maintained a constant speed of 20 m/min. This change was implemented after consultation with Dr. Bente Pedersen, senior author of the 2011 paper titled: "Exercise-induced muscle-derived cytokines inhibit mammary cancer cell growth" at University of Copenhagen, which observed an exercise induced increase of serum OSM in mice.[29]

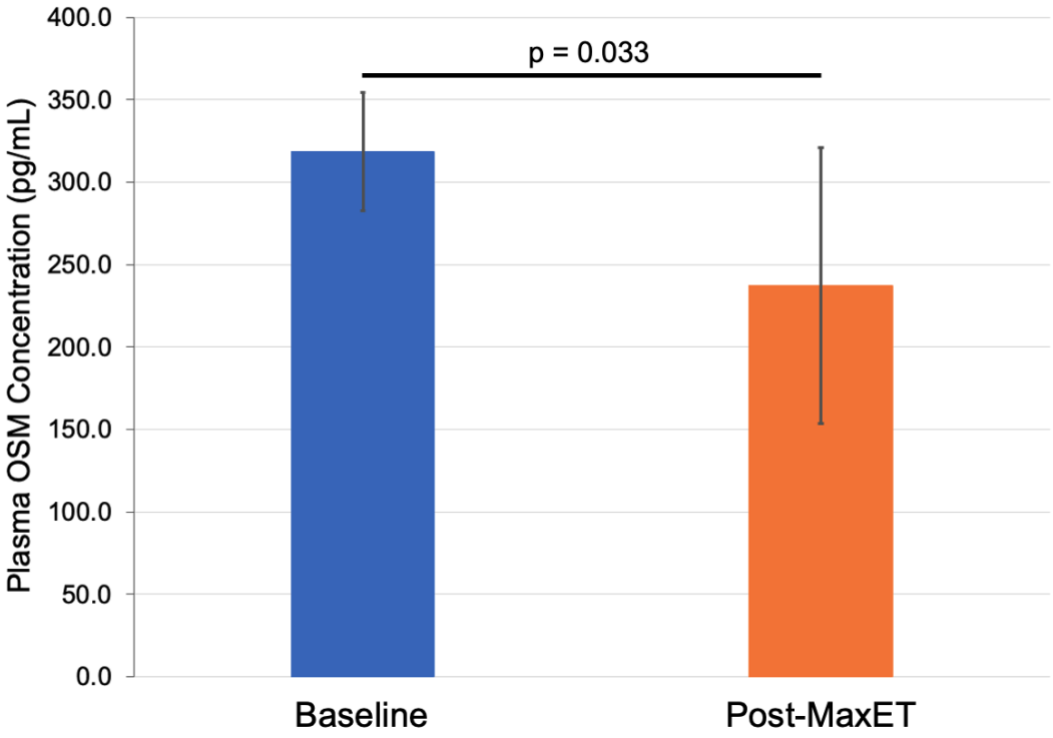

Figure **3-5**: Average Plasma OSM Concentrations before (baseline) and after MaxET (Post-MaxET). $p<0.05$. (n=6).

The parameters of the AET were further confirmed using non-tumor bearing rats from the anti-OSM pilot (n=4). These rats had not received MNU injections, and they were given a 1-month wash out period after their last anti-OSM injection prior to undergoing the AET. The post-AET plasma OSM concentrations were significantly higher (663.1±345.0 pg/mL; p=0.046) than baseline levels (241.8±19.9 pg/mL). Figure 3-6 shows the significant difference between baseline plasma OSM levels and post-AET levels from the initial pilot.

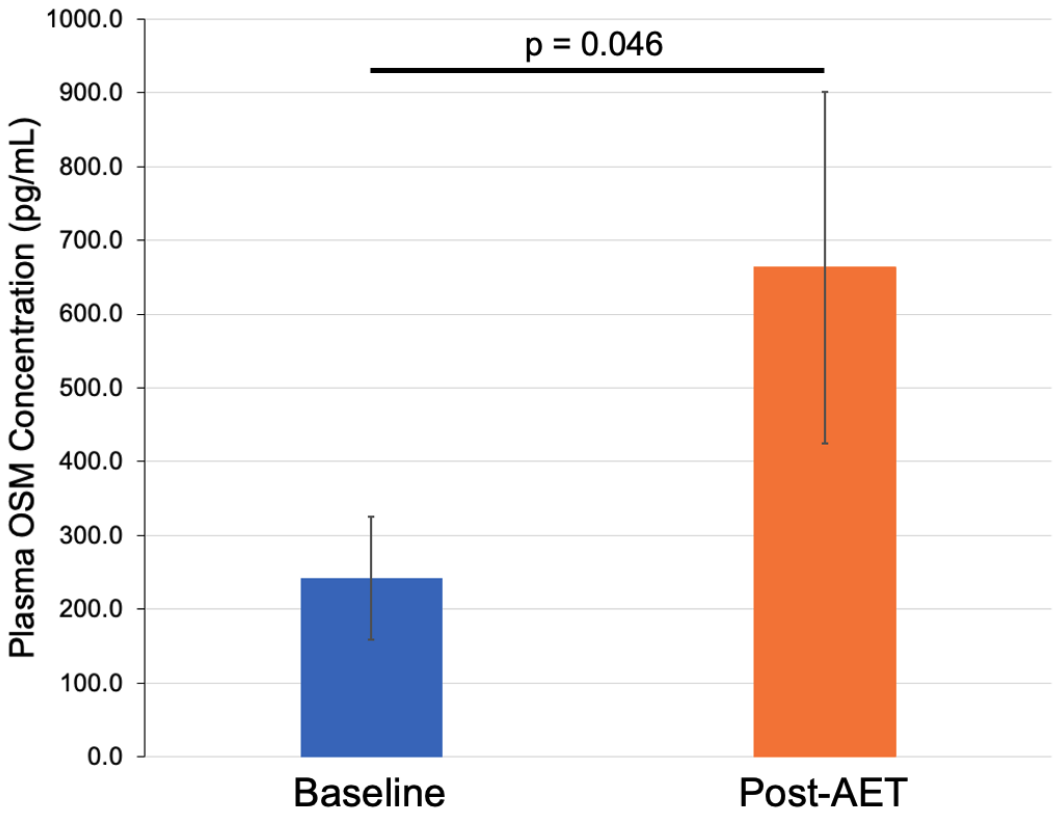

Figure **3-6**: Average Plasma OSM Concentrations before (baseline) and after AET (Post-AET). $p<0.05$. (n=4).

2. Anti-OSM Pilot Results

Plasma OSM Concentrations were not significantly different and were highly variable after single injections of 0.18 μg/rat anti-OSM or 0.9 μg/rat anti-OSM. Figure 3-7A and Figure 3-7B show plasma OSM levels over two weeks after a single injection of anti-OSM. Adverse reactions were not identified in any animals involved in this pilot after injection.

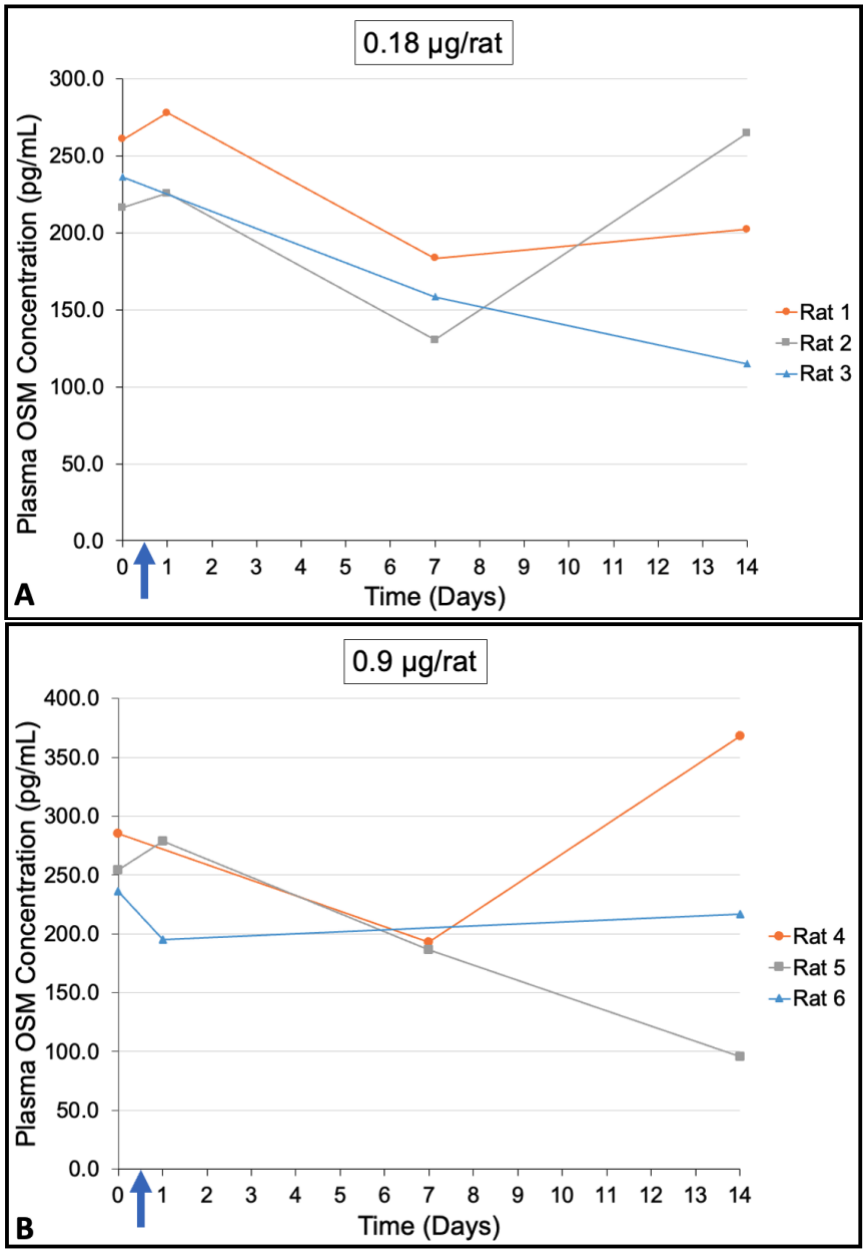

Figure **3-7**: Plasma OSM concentrations for anti-OSM pilot. A) 0.18 µg/rat anti-OSM dose, single injection. (n=3). B) 0.9 µg/rat anti-OSM dose, single injection. (n=3). Arrows indicate time of injection. No statistical significance. Each line represents an individual rat involved with pilot.

After the results of the first anti-OSM pilot were unsuccessful, an additional pilot was performed at a higher dose of anti-OSM. The groups were divided by frequency of injection, either once weekly or twice weekly. Each injection was 1.8 µg/rat. There were no significant differences in OSM plasma concentrations of any rats involved in the second pilot, and the results were also

highly variable. Figure 3-8A and Figure 3-8B show the plasma OSM levels after two weeks of injections and follow up blood draws. There were also no adverse reactions noted in any rats after the multiple injections.

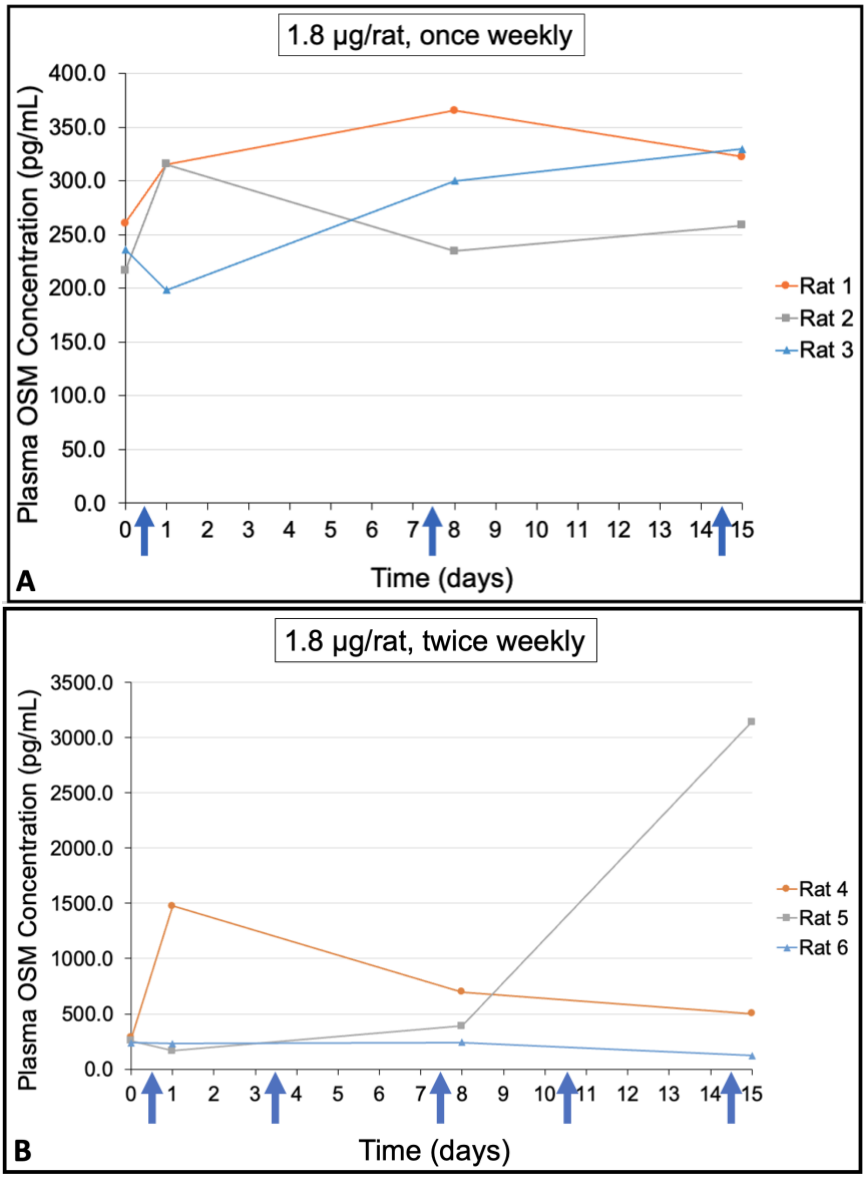

Figure **3-8**: Plasma OSM Concentrations for Anti-OSM pilot. A) 1.8 µg/rat anti-OSM dose, once weekly injection. (n=3). B) 1.8 µg/rat anti-OSM dose, twice weekly injection. (n=3). Arrows indicate time of injections. No statistical significance. Each line represents an individual rat involved with pilot.

No adverse reactions were identified in any rat for either dose or frequency within the anti-OSM pilot. Due to difficulties measuring OSM concentration, a new dose of anti-OSM was explored using supportive evidence from a mouse, *in vivo*, study. The study showed doses of 1 mg/kg IP, once weekly, was safe for administration.[37] The final dose of 50 μg/kg once weekly, IP, was extrapolated to account for lack of research regarding use of the selected antibody in rats.

3. Study Results

3.1. Animals

Rat body weights were recorded weekly with Week 0 representing the rats' pre-MNU injection weight. Figure 3-9 below shows the rat body weight growth curves for all study animals for the first 15 weeks of the study. There were no significant differences between growth curves regardless of study group intervention.

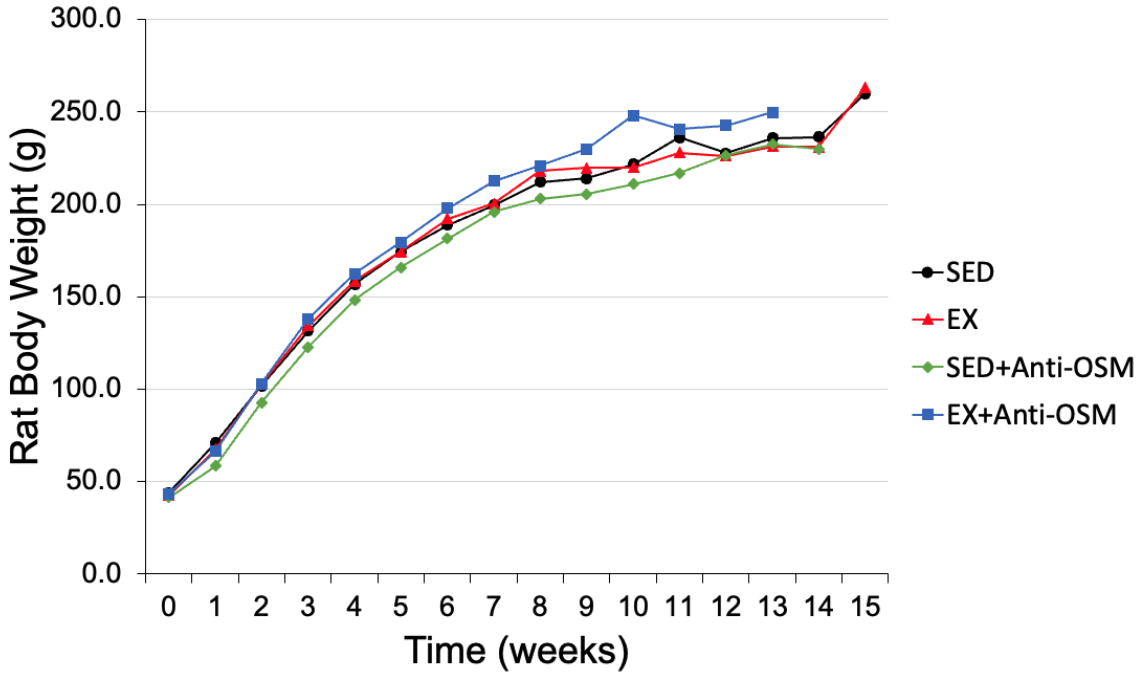

Figure **3-9**: Rat body weight growth curve over first 15 weeks. Week 0 = pre-MNU injection weight. No statistical significance. (SED n=15, EX n=15, SED+Anti-OSM n=5, EX+Anti-OSM n=13).

Heart weights were normalized to carcass weights for analysis. There were no significant differences noted between any groups when comparing heart-to-carcass weight ratio. Figure 3-10 shows the average heart-to-carcass weight ratio of all groups.

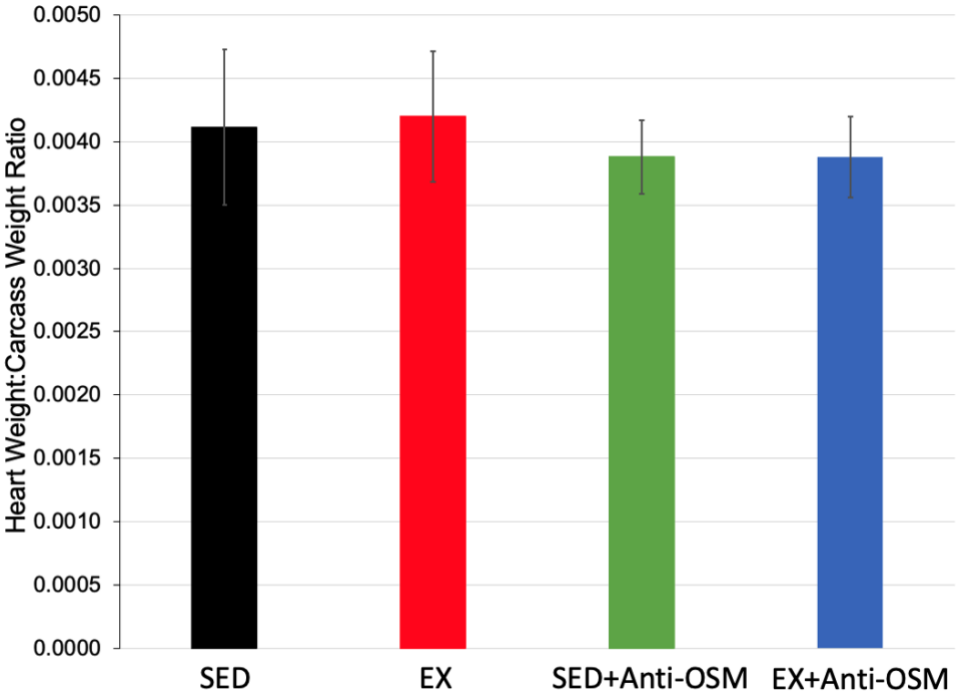

Figure **3-10**: Average heart weight to carcass weight ratio for all four groups. No statistical significance. (SED n=12, EX n=12, SED+Anti-OSM n=5, EX+Anti-OSM n=9).

3.2. Tumor Latency

Tumor latency comparisons were divided into Aim #1 and Aim #2 comparisons. Aim #1 tumor latency compared only SED and EX latency. Within SED and EX groups, one SED rat and one EX rat did not develop tumors. The same EX rat was excluded from analysis due to exercise refusal.

While EX latency was delayed (9.85±3.47 wpi), on average, compared to SED (8.28±2.20 wpi) animals, there were no significant differences between the two groups. Figure 3-11 shows this data. The survival curve also showed a longer tumor free survival time in EX rats compared to SED rats. However, the difference between groups was marginally significant (p=0.070; Figure 3-12).

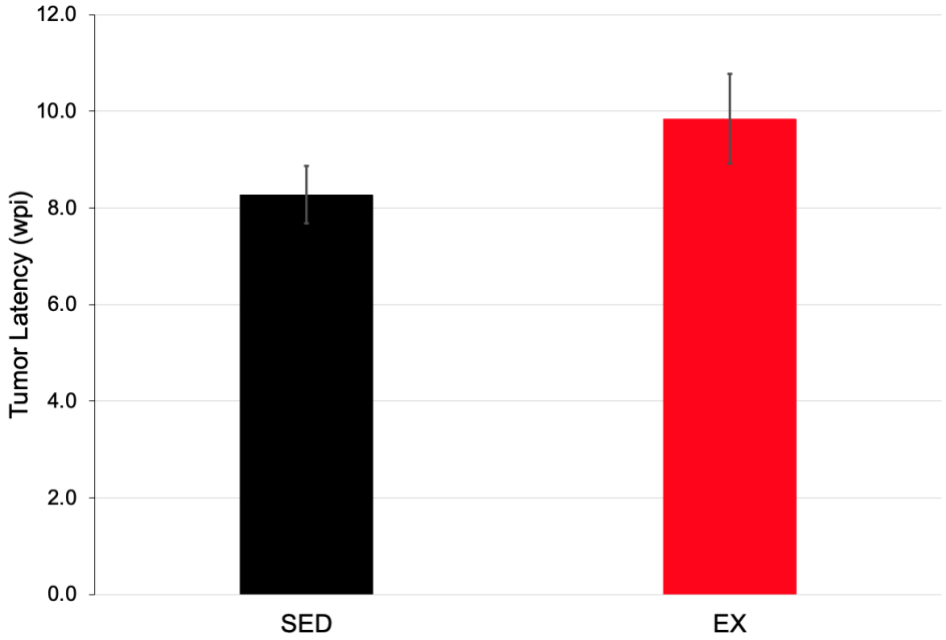

Figure **3-11**: Average tumor latency between SED and EX groups. No statistical significance. (SED n=14, EX n=14).

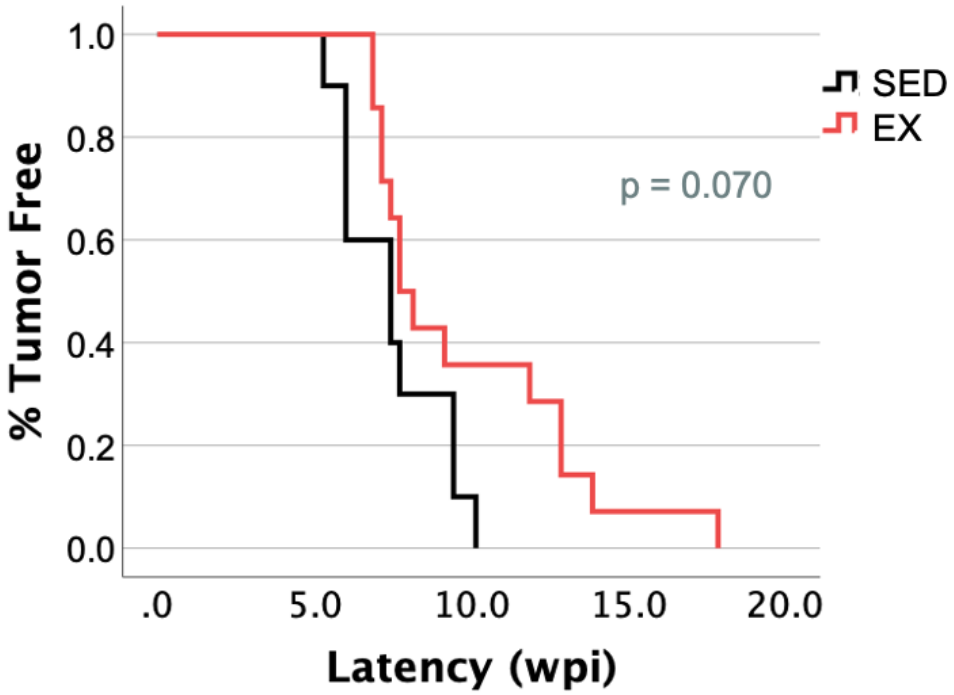

Figure **3-12**: Kaplan-Meier survival curve showing percent tumor free survival of SED and EX trained animals. $p<0.05$. (SED n=14, EX n=14).

Due to the lack of significant difference, normalized latency was calculated and analyzed. Normalized latency calculation allowed us to observe the latency without cohort variability. The calculation performed divided the latency of each rat within the cohort by the average SED latency of the cohort controls. In particular, there were two cohorts of rats (SED n=7 and EX n=5) that had potential MNU failure and potential exercise protocol variability. After normalization, there was a significant difference between SED normalized latency (1.00±0.16) and EX normalized latency (1.36±0.39; p=0.002). Figure 3-13 shows this data.

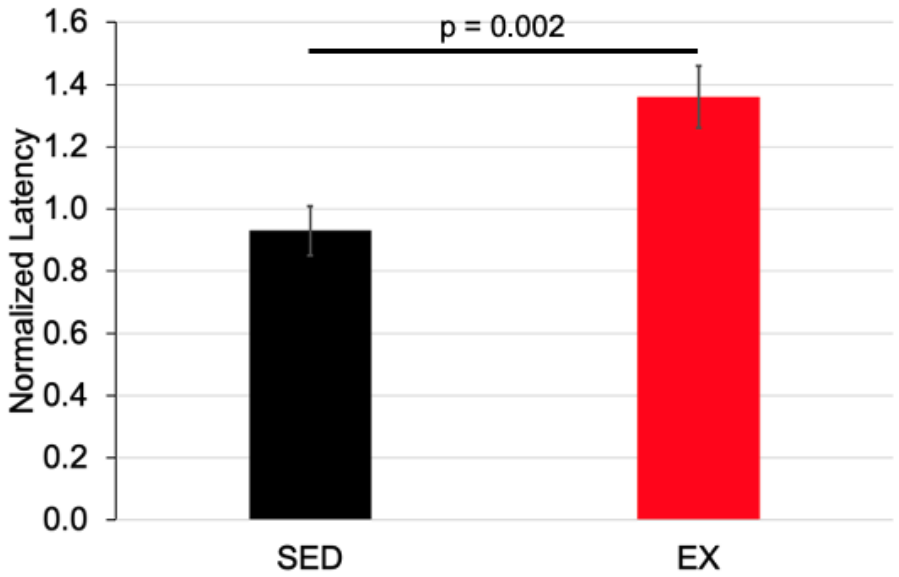

Figure **3-13**: Average normalized tumor latency between SED and EX groups. $p<0.05$. (SED n=14, EX n=14).

Aim #2 comparisons further explored the normalized latency across four experimental groups (SED, EX, SED+Anti-OSM, and EX+Anti-OSM) to observe the effect of anti-OSM on tumor latency. Three additional rats in the EX+Anti-OSM group did not develop tumors within the study timeframe. Due to difficulties with the two cohorts mentioned previously, the non-normalized data was not significantly different (data not shown). Normalized latency, however, was significantly different between EX and all other groups. Furthermore, there was no significant difference between SED, SED+Anti-OSM, or EX+Anti-OSM groups (Figure 3-14).

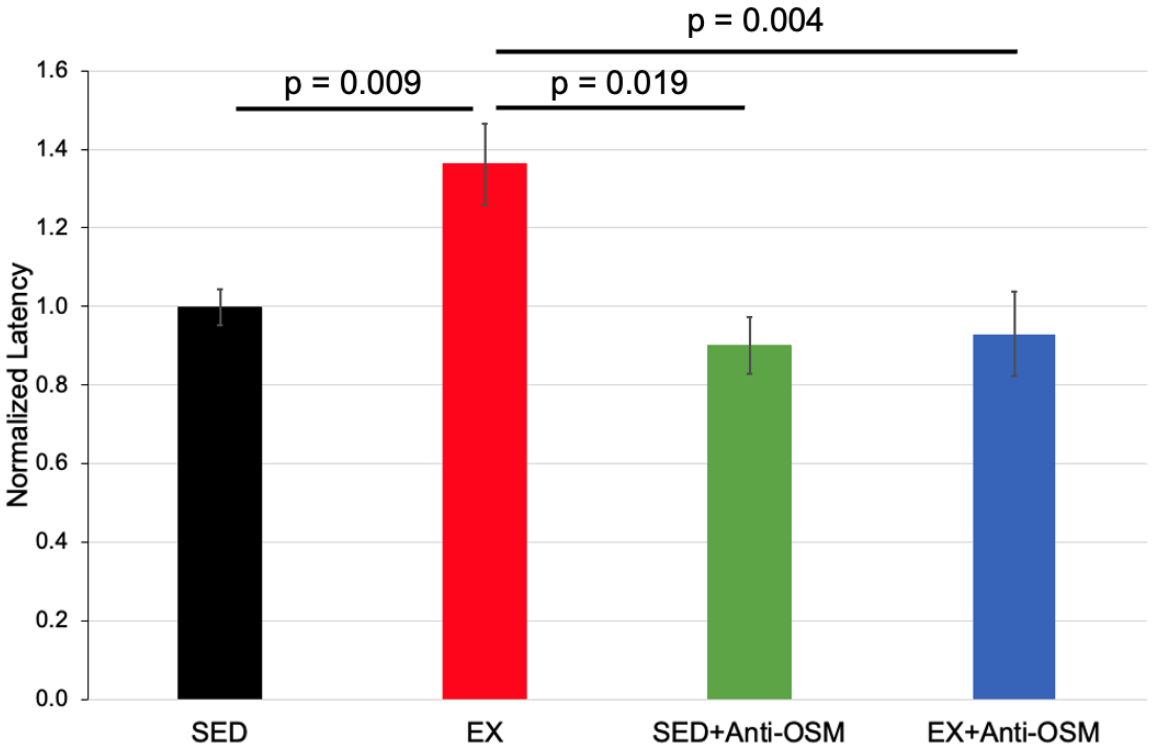

Figure **3-14**: Average normalized tumor latency for SED, EX, SED+Anti-OSM, and EX+Anti-OSM experimental groups. $p<0.05$. (SED n=14, EX n=14, SED+Anti-OSM n=5, EX+Anti-OSM n=10).

Using a 2x2 ANOVA, there was a marginally significant interaction effect for exercise and anti-OSM intervention ($p=0.08$; Figure 3-15). Cohen's D was also calculated for individual effects. A medium-to-large effect of EX on tumor latency (0.52) without normalization to SED cohort controls, and 1.20 in normalized latency. The effect of OSM in EX animals was also large at 1.53 for normalized latency (0.7 non-normalized), while OSM has a medium effect (0.43) in SED animals.

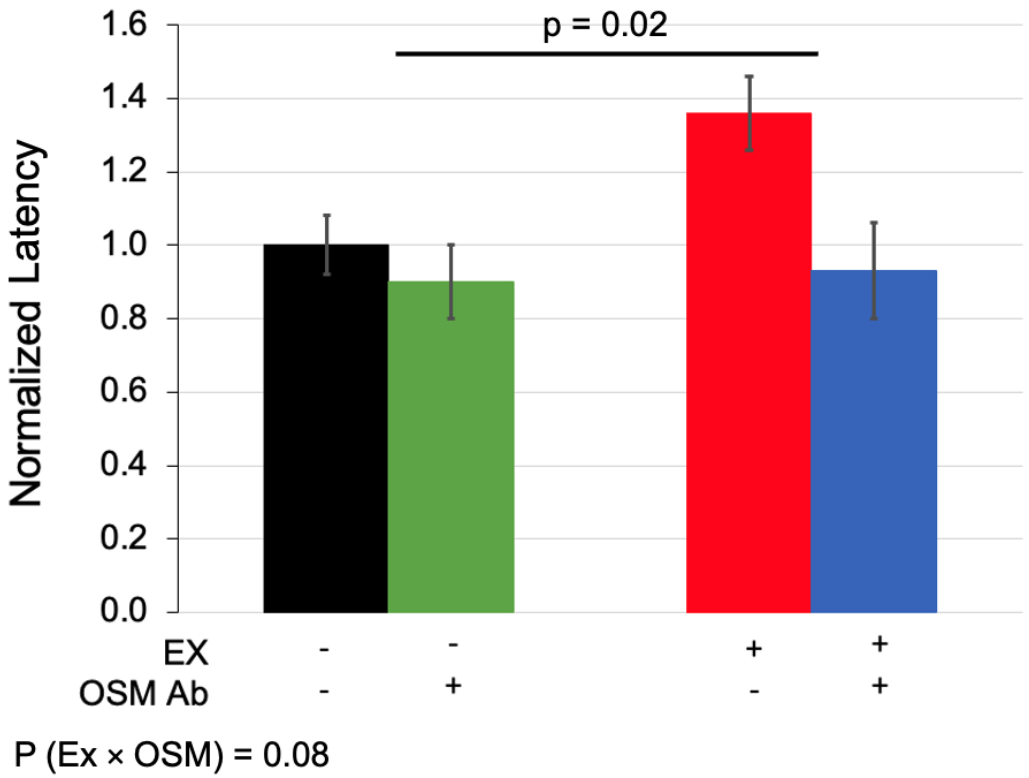

Figure **3-15**: Average normalized tumor latency for SED, EX, SED+Anti-OSM, and EX+Anti-OSM experimental groups. The interaction between EX and anti-OSM was marginally significant (p=0.08). p<0.05. (SED n=14, EX n=14, SED+Anti-OSM n=5, EX+Anti-OSM n=10).

3.3. Acute Exercise Test

Plasma OSM levels were obtained before, after, and 2 hours after the rats underwent an AET. The median plasma OSM levels of SED, non-tumor bearing rats were elevated immediately after AET, but not statistically different, as indicated by Figure 3-16. SED tumor bearing animals also demonstrated an overall elevation of plasma OSM levels immediately after AET without statistical significance. However, the plasma OSM levels did not return to baseline 2 hours later (Figure 3-17A). A similar trend was also observed for tumor bearing EX rats (Figure 3-17B). Baseline OSM concentrations for SED tumor bearing rats were higher compared to baseline OSM concentrations for EX tumor bearing rats. This difference was marginally significant (p=0.059).

Tumor bearing, EX+Anti-OSM rats did not have an increase in median plasma OSM after AET. Shown in Figure 3-18, there is a significant decrease in plasma OSM immediately after AET in the EX+Anti-OSM rats. Evaluation of tumor bearing SED+Anti-OSM plasma levels will be evaluated as a part of future studies.

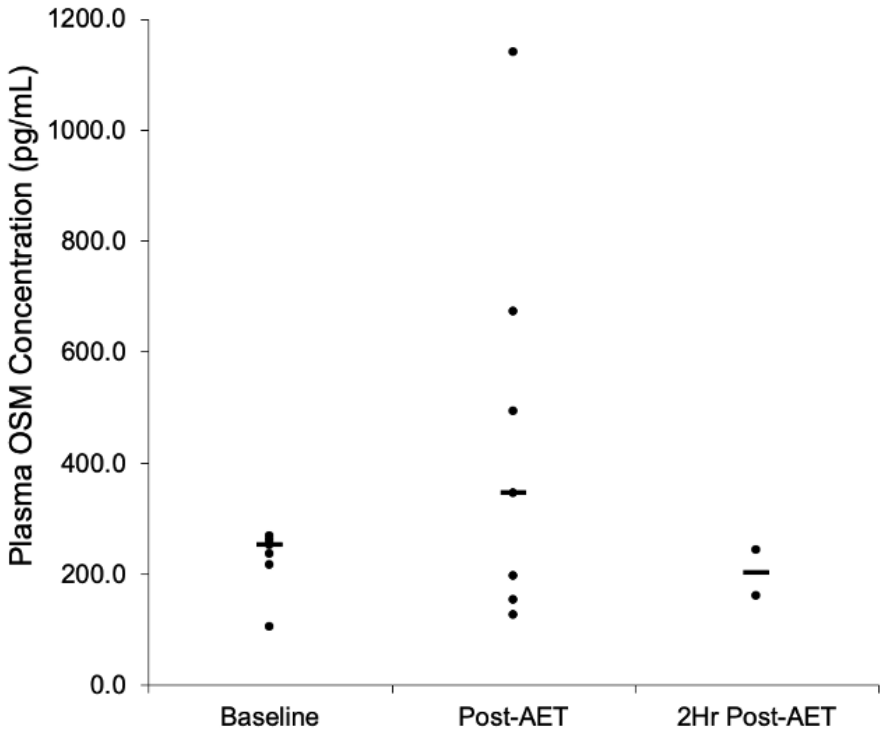

Figure **3-16**: Plasma OSM concentration before (Baseline), after (Post-AET) and 2 hours after AET (2Hr Post-AET) for non-tumor bearing SED rats. (n=7). No statistical significance. Black dash represents the median plasma OSM concentration.

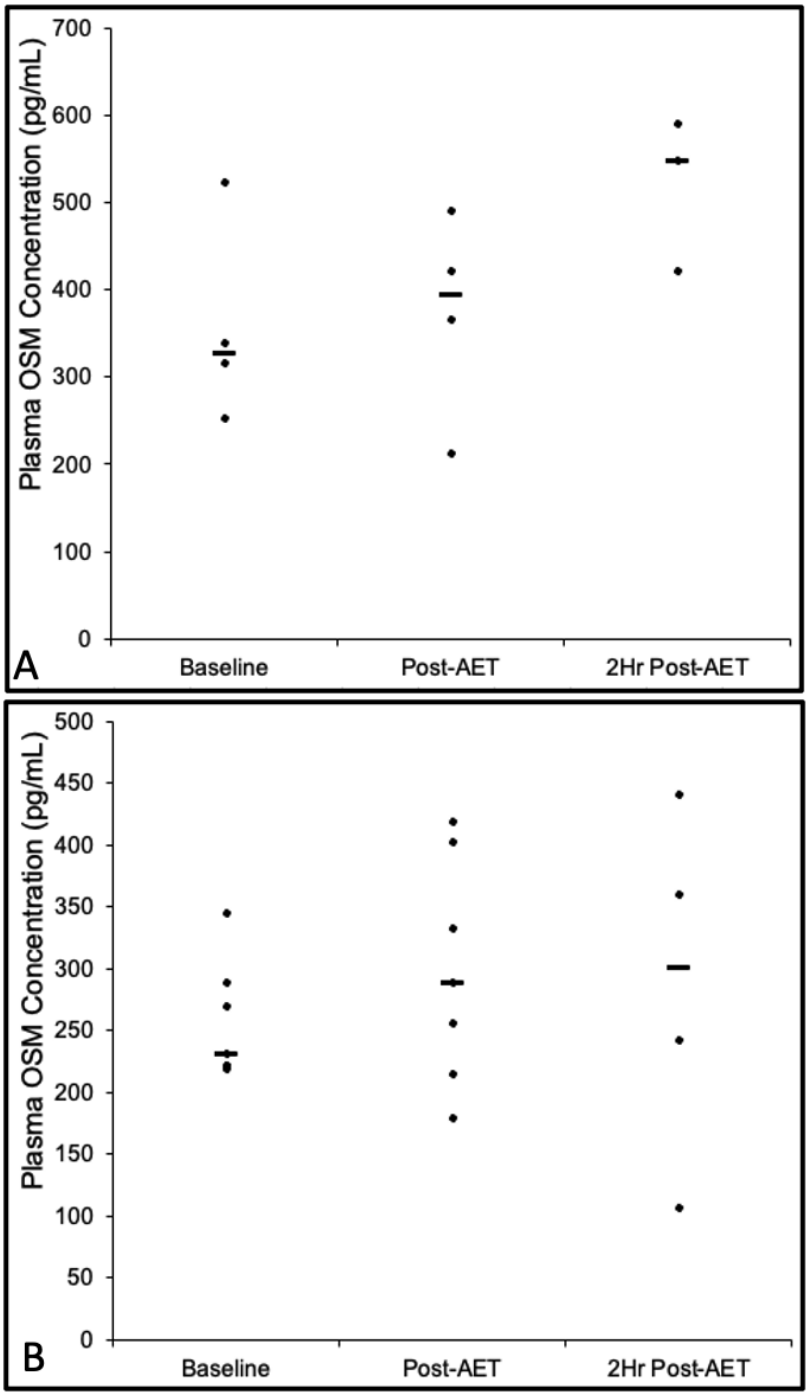

Figure **3-17**: Plasma OSM concentration before (Baseline), after (Post-AET) and 2 hours after AET (2Hr Post-AET). A) Plasma OSM concentrations for tumor bearing SED rats. (n=4). B) Plasma OSM concentrations for tumor bearing EX rats. (n=7). No statistical significance. Black dash represents the median plasma OSM concentration.

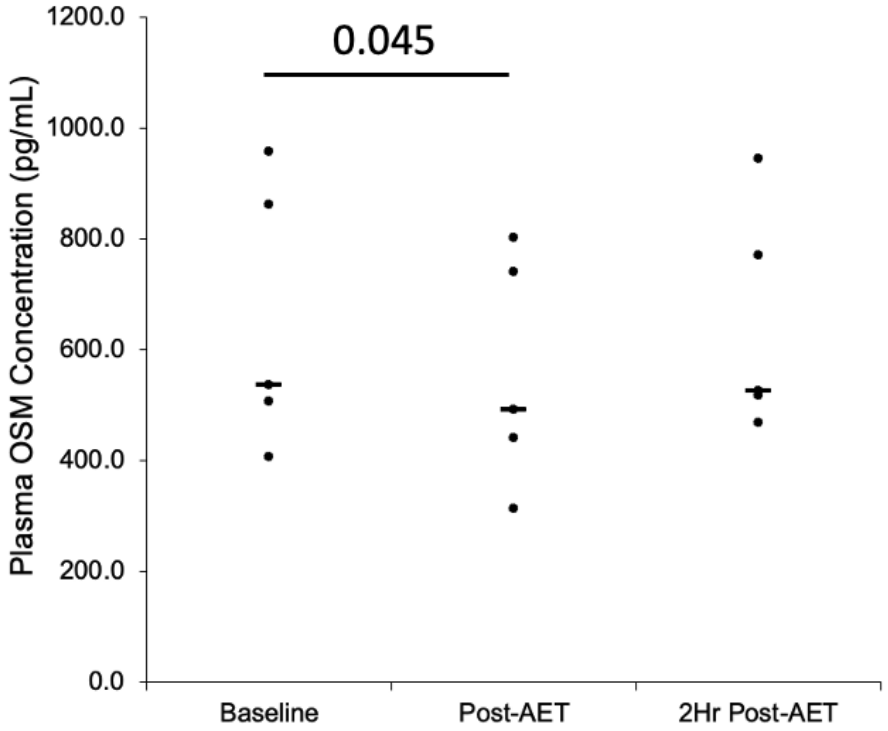

Figure **3-18**: Plasma OSM concentration before (Baseline), after (Post-AET) and 2 hours after AET (2Hr Post-AET) for tumor bearing EX+Anti-OSM rats. (n=5). $p<0.05$. Black dash represents the median plasma OSM concentration.

Due to the variability of change in plasma OSM concentrations, correlations were explored. There were no correlations between plasma OSM levels and latency, rat carcass weight, or heart weight. There was a significant negative correlation with change in plasma OSM and TTV (-0.72; p=0.001). See Figure 3-19 for the comparison. In other words, as the TTV increased, the amount of change in plasma OSM concentration was less immediately after AET.

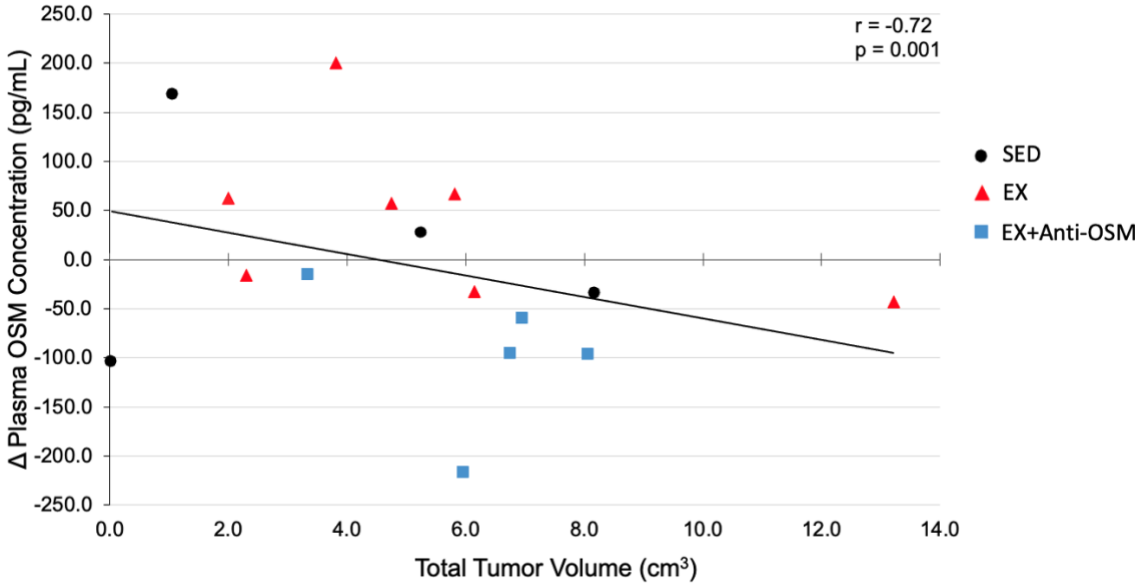

Figure **3-19**: Change in plasma OSM concentration from baseline to immediately after AET compared to total tumor volume. $p<0.05$. (SED n=4, EX n=7, EX+Anti-OSM n=5).

3.4. OSM Receptor Immunohistochemistry

OSM receptor (OSM-R) expression was also explored in both mammary tumor and the contralateral mammary chain by IHC. Both types of tissues express the protein. Representative images are shown in comparison to positive (liver) and negative (spleen) controls in Figure 3-20.

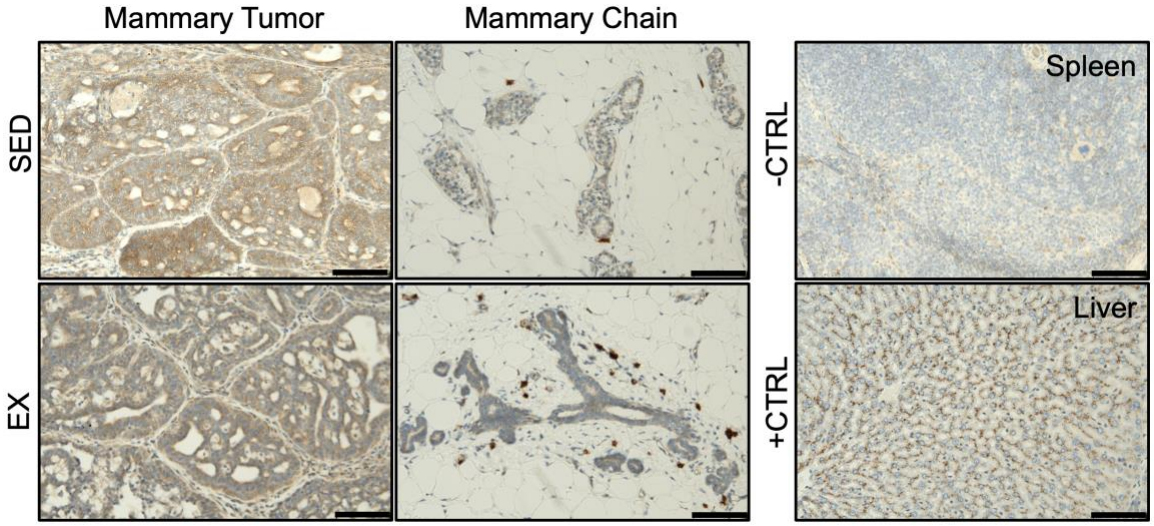

Figure **3-20**: Representative images of mammary tumor and mammary chain stained for OSM receptor. -CTRL = negative control tissue (spleen); +CTRL = positive control tissue (liver). All images taken at 20x. Scale bar = 100 μm.

Chapter 4

DISCUSSION

In the present study, we showed that exercise training delayed tumor onset in a rat model of carcinogen-induced mammary cancer. The results also demonstrated that blockade of OSM through administration of anti-OSM mitigated the protective effects of exercise training. We were unable to see a significant difference in plasma OSM changes after AET in EX rats, but we saw a marginal significance when comparing baseline OSM levels of SED and EX rats. EX rats had lower levels of OSM at baseline. Additionally, we saw an inverse relationship between changes in OSM after AET and tumor size.

MNU induction of mammary carcinogenesis in rats is a reliable and well-documented animal model for breast cancer research.[39,40] Doses of 50 mg/kg MNU IP in young (less than 35-day old) Sprague Dawley rats consistently causes development of mammary adenocarcinomas.[39,41,42] When MNU-injected rats are exercise trained, tumor onset is delayed.[4,7,41-43] We were able to show that average tumor latency for EX rats was prolonged compared to SED animals (Figure 3-11), while the effect size of exercise training was moderate (d=0.52). The lack of statistical significance was most likely due to low animal numbers causing an increase in model variation. Model accuracy depends on both MNU success in causing tumors as well as response to exercise protocol.[39,41-43] Both factors were questioned in two groups of animals due to slower tumor onset in the SED groups and minimal differences in latency between SED and EX groups. Therefore, to control for cohort variations, we explored the normalized latency of all rats. The average normalized latency of EX rats was significantly higher than SED animals (Figure 3-13). This supports the finding that there was an exercise-induced delayed latency in our MNU mammary cancer model.

Furthermore, this project sought to explore the effect of anti-OSM administration on tumor latency. In our study, anti-OSM was injected weekly into both SED and EX animals after induction of mammary cancer via MNU carcinogen. Our pilot study (see Section Chapter 3, Section 2) showed that anti-OSM could be safely administered at the manufacturer's recommended dilution in rats IP without adverse effects. Due to difficulties in observing the OSM blockade via ELISA, adjustments in the dose of anti-OSM were made based on literature searches for mouse doses and functionality tests of anti-OSM.[37,44] We suspect that the anti-OSM was binding to an epitope differing from the ELISA kit. This may have caused us to block the functionality of the peptide, but not have a noticeable difference in measurement of circulating plasma OSM.

We were able to show that relative tumor onset for EX+Anti-OSM rats was significantly shorter compared to EX rats. EX rats also had significantly longer relative latency compared to SED rats and SED+Anti-OSM rats. There were no significant differences in normalized latency of EX+Anti-OSM rats compared to SED animals or SED+Anti-OSM rats (Figure 3-14). This suggests that OSM blockade of EX animals causes latencies similar to SED animals, while OSM blockade does not impact latency in rats that are sedentary. Additionally, the effect size showed that anti-OSM had a lesser effect on latency of SED animals (d=0.49), but a large effect in EX animals (d=1.53). This supports our hypothesis that anti-OSM would mitigate the effect of exercise in breast cancer prevention. However, this refutes our hypothesis that anti-OSM would accelerate tumor onset in SED animals.

There are few studies regarding the exploration of the OSM pathway in reference to breast cancer prevention, *in vivo*.[32] Previous studies have shown the impact of OSM on breast cancer cells, *in vitro*.[29,45] Post-exercise serum from mice was used by Hojman *et al* to culture the MCF-7 breast cancer cell line. Serum from mice immediately post-exercise caused increased caspase activity and decreased cell proliferation. Exploration of gene expression revealed several possible myokines and acute factors within the serum that could have contributed to this phenomenon. The group then

moved on to culture MCF-7 cells with serum rich with either OSM, IL-10, IL-11, or growth differentiation factor 5 (GDF5). OSM rich serum caused statistically significant slower cell growth in the MCF-7 cells compared to control cells, while the other cytokines tested did not change the cell growth.[29]

Previously, groups have also explored the OSM pathway through interruption of different parts of the mechanism. OSM-R blockade has been performed in a variety of genetically modified OSM-R knockout mice in order to explore the effects on cellular processes, such as hematopoesis and cardiomyocyte differentiation.[46,47] In both Tanaka *et al* and Kubin *et al*, OSM-R knockout mice were developed using homologous recombination in embryonic stem cells. Tanaka *et al* was able to show the role of OSM in regulating hematopoesis through stromal cell and progenitor stimulation. Kubin *et al* was able to show that suppression of OSM mechanisms decreases cardiomyocyte remodeling after myocardial infarction.[32,46,47]

Contradictory to our findings, Araujo *et al*, found that knocking out the OSM-R in a mouse model of mammary cancer halted tumor progression. Their study suggests that OSM expressed in the breast cancer stroma may play a role in promoting tumor progression.[32] Looking at the data from the Araujo *et al* study in combination with the results of this thesis, there is some support that although OSM prevents tumor development, the role of OSM is likely dependent on the stage of cancer.

Our goal to interrupt the effect of the OSM peptide through administration of anti-OSM was novel in regard to breast cancer in rats. Anti-OSM administration to mice has been explored in other diseases such as lupus nephritis and arthritis.[37,44] A dose of 1mg/kg anti-OSM IP, once weekly over a 4-week study in a mouse model of systemic lupus erythematosus, ameliorated the effects of the disease specifically related to tubulointerstitial damage of the kidney.[37] Similarly, one group found that two IP injections, separated by two days, of anti-OSM at 100 μg/mouse may be a promising therapeutic target for rheumatoid arthritis.[44] Anti-OSM has also been explored in clinical

trials of humans with rheumatoid arthritis.[48] The study showed that intravenous doses of anti-OSM is safe for humans, however, there was limited efficacy of the antibody. The group suggested exploring higher affinity anti-OSM to improve the clinical effect.[48]

Previous studies have not explored the effect of exercise training on OSM release by skeletal muscle in rats. Plasma OSM levels increased after AET for some rats as we would expect (Figures 3-16 and 3-17). However, there was noticeable variability in the degree of change for our study. There was also variability where some rats had a decrease in plasma OSM concentration post-AET (Figure 3-18). Additionally, baseline levels of OSM in tumor bearing SED animals were higher than tumor bearing EX animals with marginal significance ($p=0.059$). We expected the results of this study to show EX rats having a larger change in plasma OSM after AET compared to SED rats, and EX rats would have higher baseline levels compared to SED rats. One study suggests that serum OSM increased immediately after acute exercise in experimentally naïve mice.[29] OSM patterns were not explored in tumor-bearing animals. It has also been shown that IL-6 levels decrease with endurance training.[22] It is possible that since IL-6 and OSM are within the same cytokine family, their response to exercise training is similar. Additional non-tumor bearing rats should be analyzed in order to further elucidate this pattern.

Since our original hypothesis regarding AET and plasma OSM levels could not be supported, correlations were explored to compare plasma OSM levels with TTV, primary TV, and latency. Correlations suggest that TTV may impact the degree of change in plasma OSM levels after acute exercise. Our results show that rats with smaller tumor volume at the time of AET had larger changes in plasma OSM immediately following AET compared to their baseline values (Figure 3-19). We suspect that the results of this correlation may be related to cancer cachexia, although the mechanism behind this is not apparent at this time. Our first speculation is that as the muscle atrophies with cancer cachexia, OSM release could be inhibited due to altered metabolic pathways.[49,50] Cancer cachexia is also exacerbated by tumor amino acid requirements. As muscle

breaks down, additional amino acids are available for tumor uptake.[49] An additional possibility for these changes relates to increased OSM binding to OSM-R with muscle breakdown in a similar fashion.[49] If the latter scenario can be supported, additional connections could be made regarding OSM within the tumor microenvironment.[32] Further analysis of tumor sizes and changes in OSM are required to better classify this unexpected difference.

Despite the findings of this study, the experiment was not without limitations. The first limitation in the study was in regard to two specific cohorts of rats. The rats of these two groups had high variability in latency. We suspect that there were two reasons for this: MNU failure and high variability in the running compliance protocol for the rats. MNU failure likely led to SED rats developing tumors that ultimately did not grow, and one SED rat did not develop a tumor at all. Three separate experimenters were responsible for executing the daily treadmill protocol for the two groups of rats in question. It is highly likely that having more than one experimenter decreased the effect of exercise on latency due to variability in enforcing running.

Another limitation to the study was the lack of functionality test for anti-OSM. Current publications that involve systemic administration of anti-OSM to rodents do not describe benchtop tests that are able to assess functionality of the OSM peptide after blockade. Rather, the groups describe the effect of the anti-OSM on a particular disease process after administration.[37,44] The ELISA kit that was selected was able to detect circulating OSM levels, however, we were unable to distinguish a functional effect other than changes in tumor latency.

There is also a general lack of knowledge regarding the OSM response in rats; this created a limitation in evaluating plasma OSM release following AET. There are currently no studies available that offer species differences for OSM release after exercise. Hojman *et al*, showed that mice following a 60-minute forced swim test have significantly increased serum OSM concentrations.[29] The difference in species between studies may have an impact. Additionally, the form of exercise could have impacted the results. Since OSM is a part of the IL-6 cytokine family,

it is known that OSM response may be enhanced in the face of glucocorticoid stress.[51] One hypothesis for the variability was that treadmill trained rats may elicit a different stress response compared to the forced swim test, due to all rats in our study being familiar with the treadmill. Therefore, the response of OSM may require different exercise parameters to consistently elicit OSM release after running on a motorized treadmill. Additional experiments would be required to determine the difference between elevation of OSM secondary to exercise or acute stressors.

To our knowledge, this is the first study demonstrating that weekly injections of anti-OSM in rats with carcinogen induced mammary cancer mitigates the exercise effect on tumor latency. Correlations between changes in plasma OSM and tumor burden have not been described in the literature. The basis of these findings suggests that OSM release from the muscle during exercise is an important factor in the mechanism driving exercise-induced breast cancer prevention. The results of this study in combination with future studies will lay groundwork for developing novel chemo-prevention strategies in women who are unable or unwilling to exercise.

Chapter 5

CONCLUSIONS AND FUTURE DIRECTIONS

In conclusion, this study suggests that OSM release from muscles into systemic circulation after exercise plays a role in delaying tumor development in a carcinogen-induced mammary cancer rat model. We were able to demonstrate that exercise caused delay in tumor onset compared to SED animals, and we also showed that the administration of anti-OSM mitigated this effect. Although we were unable to consistently observe an increase in plasma OSM immediately following AET, we saw that the TTV may impact this change.

Limitations in the current study warrant further exploration of several items including: 1) acute treadmill exercise in additional experimentally naïve, adult, female Sprague Dawley rats, 2) exploration and identification of functional assays for OSM, and 3) exploration of the effect on corticosterone on OSM release. This information is pertinent in classifying OSM patterns in female rats after acute or chronic exercise.

Future evaluations that were not completed in this study should observe correlations between tumor growth rate and anti-OSM administration. This would show whether anti-OSM impacts tumor growth after it has developed, as some studies suggest the presence of OSM may drive breast cancer tumor progression.[32] Similarly, OSM-R immunohistochemistry should be evaluated for differences between EX and SED rats. Our current samples show that OSM-R is expressed in both mammary tumor and mammary chain. A semi-quantitative measurement may provide insight to the relationship between OSM and OSM-R in these tissues. Thus, further differentiating the therapeutic significance of OSM at different stages of cancer. Administration of recombinant OSM to SED animals would also provide guidance for potential therapeutic targets. Our group was able to show the effects of anti-OSM in the cancer initiation phase of a breast cancer

model. Next steps should observe how tumor latency changes when SED animals are administered OSM compared to EX animals.

As the breast cancer incidence rate increases, research involving prevention strategies become increasingly more important. OSM studies should focus on differentiating between beneficial and detrimental effects of the myokine on breast cancer. Further exploration of the impact on breast cancer initiation and progression by physical activity induced OSM release is critical for identifying therapeutic targets in women who are not physically active.

REFERENCES

1. Siegel RL, Miller KD, Fuchs HE, et al. Cancer Statistics, 2021. CA Cancer J Clin 2021;71:7-33.
2. de Boer MC, Worner EA, Verlaan D, et al. The Mechanisms and Effects of Physical Activity on Breast Cancer. Clin Breast Cancer 2017;17:272-278.
3. Sun YS, Zhao Z, Yang ZN, et al. Risk Factors and Preventions of Breast Cancer. Int J Biol Sci 2017;13:1387-1397.
4. Faustino-Rocha AI, Gama A, Oliveira PA, et al. Effects of lifelong exercise training on mammary tumorigenesis induced by MNU in female Sprague-Dawley rats. Clin Exp Med 2017;17:151-160.
5. Britt KL, Cuzick J, Phillips KA. Key steps for effective breast cancer prevention. Nat Rev Cancer 2020;20:417-436.
6. Li Y. Potential Mechanisms behind Physical Exercise vs. Epigenetic Regulation for Preventing Breast Cancer. Journal of Cancer Prevention & Current Research 2017;8.
7. Sturgeon KM, Schweitzer A, Leonard JJ, et al. Physical activity induced protection against breast cancer risk associated with delayed parity. Physiol Behav 2017;169:52-58.
8. McDonald ES, Clark AS, Tchou J, et al. Clinical Diagnosis and Management of Breast Cancer. J Nucl Med 2016;57 Suppl 1:9S-16S.
9. Mariotto AB, Yabroff KR, Shao Y, et al. Projections of the cost of cancer care in the United States: 2010-2020. J Natl Cancer Inst 2011;103:117-128.
10. Ballard-Barbash R, Friedenreich CM, Courneya KS, et al. Physical Activity, Biomarkers, and Disease Outcomes in Cancer Survivors: A Systematic Review. J Natl Cancer Inst 2012;104:815-840.
11. Wu Y, Zhang D, Kang S. Physical activity and risk of breast cancer: a meta-analysis of prospective studies. Breast Cancer Res Treat 2013;137:869-882.
12. Neilson HK, Conroy SM, Friedenreich CM. The Influence of Energetic Factors on Biomarkers of Postmenopausal Breast Cancer Risk. Curr Nutr Rep 2014;3:22-34.
13. Wang Q, Zhou W. Roles and molecular mechanisms of physical exercise in cancer prevention and treatment. J Sport Health Sci 2021;10:201-210.
14. Hong BS, Lee KP. A systematic review of the biological mechanisms linking physical activity and breast cancer. Phys Act Nutr 2020;24:25-31.
15. Patel AV, Friedenreich CM, Moore SC, et al. American College of Sports Medicine Roundtable Report on Physical Activity, Sedentary Behavior, and Cancer Prevention and Control. Med Sci Sports Exerc 2019;51:2391-2402.
16. McTiernan A. Mechanisms linking physical activity with cancer. Nat Rev Cancer 2008;8:205-211.
17. Ruiz-Casado A, Martin-Ruiz A, Perez LM, et al. Exercise and the Hallmarks of Cancer. Trends Cancer 2017;3:423-441.
18. Goncalves AK, Dantas Florencio GL, Maisonnette de Atayde Silva MJ, et al. Effects of physical activity on breast cancer prevention: a systematic review. J Phys Act Health 2014;11:445-454.
19. Laurens C, Bergouignan A, Moro C. Exercise-Released Myokines in the Control of Energy Metabolism. Front Physiol 2020;11:91.

20. Gomarasca M, Banfi G, Lombardi G. Myokines: The endocrine coupling of skeletal muscle and bone. Adv Clin Chem 2020;94:155-218.
21. Richards CD. The enigmatic cytokine oncostatin m and roles in disease. ISRN Inflamm 2013;2013:512103.
22. Severinsen MCK, Pedersen BK. Muscle-Organ Crosstalk: The Emerging Roles of Myokines. Endocr Rev 2020;41:594-609.
23. Hutt JA, Dewille JW. Oncostatin M Induces Growth Arrest of Mammary Epithelium via a CCAAT/enhancer-binding Protein delta-dependent Pathway. Molecular Cancer Therapeutics 2002;1:601-610.
24. Rose-John S. Interleukin-6 Family Cytokines. Cold Spring Harb Perspect Biol 2018;10.
25. Grant SL, Begley CG. The oncostatin M signalling pathway: reversing the neoplastic phenotype? Molecular Medicine Today 1999;5:406-412.
26. Chen M, Ren R, Lin W, et al. Exploring the oncostatin M (OSM) feed-forward signaling of glioblastoma via STAT3 in pan-cancer analysis. Cancer Cell Int 2021;21:565.
27. Dey G, Radhakrishnan A, Syed N, et al. Signaling network of Oncostatin M pathway. J Cell Commun Signal 2013;7:103-108.
28. Komori T, Morikawa Y. Essential roles of the cytokine oncostatin M in crosstalk between muscle fibers and immune cells in skeletal muscle after aerobic exercise. J Biol Chem 2022;298:102686.
29. Hojman P, Dethlefsen C, Brandt C, et al. Exercise-induced muscle-derived cytokines inhibit mammary cancer cell growth. Am J Physiol Endocrinol Metab 2011;301:E504-510.
30. Hwang JH, McGovern J, Minett GM, et al. Mobilizing serum factors and immune cells through exercise to counteract age-related changes in cancer risk. Exerc Immunol Rev 2020;26:80-99.
31. Goj T, Hoene M, Fritsche L, et al. The Acute Cytokine Response to 30-Minute Exercise Bouts Before and After 8-Week Endurance Training in Individuals With Obesity. J Clin Endocrinol Metab 2023;108:865-875.
32. Araujo AM, Abaurrea A, Azcoaga P, et al. Stromal oncostatin M cytokine promotes breast cancer progression by reprogramming the tumor microenvironment. J Clin Invest 2022;132.
33. Tawara K, Bolin C, Koncinsky J, et al. OSM potentiates preintravasation events, increases CTC counts, and promotes breast cancer metastasis to the lung. Breast Cancer Res 2018;20:53.
34. Masjedi A, Hajizadeh F, Beigi Dargani F, et al. Oncostatin M: A mysterious cytokine in cancers. Int Immunopharmacol 2021;90:107158.
35. Noh J, You C, Kang K, et al. Activation of OSM-STAT3 Epigenetically Regulates Tumor-Promoting Transcriptional Programs in Cervical Cancer. Cancers (Basel) 2022;14.
36. Research IfLA. Guide for the Care and Use of Laboratory Animals, 8th edThe National Academies Press; 2011.
37. Liu Q, Du Y, Li K, et al. Anti-OSM Antibody Inhibits Tubulointerstitial Lesion in a Murine Model of Lupus Nephritis. Mediators Inflamm 2017;2017:3038514.
38. Faustino-Rocha A, Oliveira PA, Pinho-Oliveira J, et al. Estimation of rat mammary tumor volume using caliper and ultrasonography measurements. Lab Animal 2013;42:217-224.
39. Thompson HJ, Adlakha H, Singh M. Effect of carcinogen dose and age at administration on induction of mammary carcinogenesis by 1-methyl-1-nitrosourea. Carcinogenesis 1992;13:1535-1539.
40. Zeng L, Li W, Chen CS. Breast cancer animal models and applications. Zool Res 2020;41:477-494.
41. Thompson HJ. Effects of physical activity and exercise on experimentally-induced mammary carcinogenesis. Breast Cancer Res Treat 1997;46:165-141.

42. Thompson HJ, Westerlind KC, Snedden J, et al. Exercise intensity dependent inhibition of 1-methyl-1-nitrosourea induced mammary carcinogenesis in female F-344 rats. Carcinogenesis 1995;16:1783-1786.
43. Thompson HJ, Westerlind KC, Snedden J, et al. Inhibition of Mammary Carcinogenesis by Treadmill Exercise. Journal of National Cancer Institute 1995;87:453-455.
44. Plater-Zyberk C, Buckton J, Thompson S, et al. Amelioration of arthritis in two murine models using antibodies to oncostatin M. Arthritis Rheum 2001;44:2697-2702.
45. Kucia-Tran JA, Tulkki V, Scarpini CG, et al. Anti-oncostatin M antibody inhibits the pro-malignant effects of oncostatin M receptor overexpression in squamous cell carcinoma. J Pathol 2018;244:283-295.
46. Tanaka M, Hirabayashi Y, Sekiguchi T, et al. Targeted disruption of oncostatin M receptor results in altered hematopoiesis. Blood 2003;102:3154-3162.
47. Kubin T, Poling J, Kostin S, et al. Oncostatin M is a major mediator of cardiomyocyte dedifferentiation and remodeling. Cell Stem Cell 2011;9:420-432.
48. Choy EH, Bendit M, McAleer D, et al. Safety, tolerability, pharmacokinetics and pharmacodynamics of an anti-oncostatin M monoclonal antibody in rheumatoid arthritis: results from phase II randomized, placebo-controlled trials. Arthritis Res Ther 2013;15.
49. Peixoto da Silva S, Santos JMO, Costa ESMP, et al. Cancer cachexia and its pathophysiology: links with sarcopenia, anorexia and asthenia. J Cachexia Sarcopenia Muscle 2020;11:619-635.
50. Bilgic SN, Domaniku A, Toledo B, et al. EDA2R-NIK signalling promotes muscle atrophy linked to cancer cachexia. Nature 2023;617:827-834.
51. G.J. W, Reul JMHM. Induction of cytokine receptors by glucocorticoids: functional and pathological significance. Trends in Pharmacological Sciences 1998;19:317-321.